

Long-term Particulate Matter Modeling for Health Effects Studies in California – Part I: Model Performance on Temporal and Spatial Variations

*Jianlin Hu¹, Hongliang Zhang¹, Qi Ying², Shu-Hua Chen³, Francois Vandenberghe⁴, and
Michael J. Kleeman^{1*}*

*¹Department of Civil and Environmental Engineering, University of California, Davis. One
Shields Avenue, Davis CA. ²Zachry Department of Civil Engineering, Texas A&M University,
College Station TX. ³Department of Land, Air, and Water Resources, University of California,
Davis. One Shields Avenue, Davis, CA. ⁴Research Applications Laboratory, National Center for
Atmospheric Research, Boulder, CO.*

**Corresponding author. Tel.: +1 530 752 8386; fax; +1 530 752 7872. E-mail address:
mjkleeman@ucdavis.edu (M.J. Kleeman).*

2 **Abstract**

3 For the first time, a ~decadal (9 years from 2000 to 2008) air quality model simulation
4 with 4 km horizontal resolution over populated regions and daily time resolution has been
5 conducted for California to provide air quality data for health effects studies. Model predictions
6 are compared to measurements to evaluate the accuracy of the simulation with an emphasis on
7 spatial and temporal variations that could be used in epidemiology studies. Better model
8 performance is found at longer averaging times, suggesting that model results with averaging
9 times ≥ 1 month should be the first to be considered in epidemiological studies. The UCD/CIT
10 model predicts spatial and temporal variations in the concentrations of O₃, PM_{2.5}, elemental
11 carbon (EC), organic carbon (OC), nitrate, and ammonium that meet standard modeling
12 performance criteria when compared to monthly-averaged measurements. Predicted sulfate
13 concentrations do not meet target performance metrics due to missing sulfur sources in the
14 emissions. Predicted seasonal and annual variations of PM_{2.5}, EC, OC, nitrate, and ammonium
15 have mean fractional biases that meet the model performance criteria in 95%, 100%, 71%, 73%,
16 and 92% of the simulated months, respectively. The base dataset provides an improvement for
17 predicted population exposure to PM concentrations in California compared to exposures
18 estimated by central site monitors operated one day out of every 3 days at a few urban locations.

19 Uncertainties in the model predictions arise from several issues. Incomplete
20 understanding of secondary organic aerosol formation mechanisms leads to OC bias in the model
21 results in summertime but does not affect OC predictions in winter when concentrations are
22 typically highest. The CO and NO (species dominated by mobile emissions) results reveal
23 temporal and spatial uncertainties associated with the mobile emissions generated by the
24 EMFAC 2007 model. The WRF model tends to over-predict wind speed during stagnation

25 events, leading to under-predictions of high PM concentrations, usually in winter months. The
26 WRF model also generally under-predicts relative humidity, resulting in less particulate nitrate
27 formation, especially during winter months. These limitations must be recognized when using
28 data in health studies. All model results included in the current manuscript can be downloaded
29 free of charge at <http://faculty.engineering.ucdavis.edu/kleeman/>.

30 **Key Words:** particulate matter, chemical transport models, temporal variation, spatial variation

31 **1. Introduction**

32
33 Numerous scientific studies have demonstrated associations between exposure to ambient
34 airborne particulate matter (PM) and a variety of health effects, such as cardiovascular diseases
35 (Dockery, 2001; Ford et al., 1998; Franchini and Mannucci, 2009; Langrish et al., 2012; Le
36 Tertre et al., 2002), respiratory diseases (Gordian et al., 1996; Hacon et al., 2007; Hughes and
37 Tolsma, 2002; Willers et al., 2013), low birth weight and birth defects (Barnett et al., 2011; Bell
38 et al., 2010; Brauer et al., 2008; Laurent et al., 2014; Laurent et al., 2013; Stieb et al., 2012), lung
39 cancer (Beelen et al., 2008; Beeson et al., 1998; Pope et al., 2002; Vineis et al., 2006), mortality
40 and life expectancy (Chen et al., 2013; Correia et al., 2013; Dockery et al., 1993; Franklin et al.,
41 2007; Goldgewicht, 2007; Kan and Gu, 2011; Laden et al., 2000; Ostro et al., 2006; Pope et al.,
42 2009). Recently a few studies have investigated the associations between particle composition
43 and health effects (Bell et al., 2010; Bell et al., 2007; Burnett et al., 2000; Cao et al., 2012;
44 Franklin et al., 2008; Ito et al., 2011; Krall et al., 2013; Levy et al., 2012; Mar et al., 2000; Ostro
45 et al., 2007; Ostro et al., 2010; Son et al., 2012). However, there remains large uncertainty about
46 which PM components are most responsible for the observed health effects, possibly due to the
47 fact that central site monitoring measurements used in the PM composition studies have limited

48 temporal, spatial, and chemical resolution, which could potentially lead to misclassification of
49 exposure estimates and mask some detailed correlations. Central site PM measurements typically
50 have a collection schedule of 1 sample every 3 or 6 days at a few sites used to represent an entire
51 population region. Important particle size distribution and chemical composition information is
52 not always routinely measured. Additional information relating PM composition to health effects
53 would provide a solid foundation to design effective PM control strategies to protect public
54 health at a reduced economic and social cost.

55
56 Chemical transport models (CTMs) have recently been used as one of the alternative
57 approaches to address the limitations of central site monitors (Anenberg et al., 2010; Bravo et al.,
58 2012; Sarnat et al., 2011; Tainio et al., 2012). The latest generation of CTMs represents a “state-
59 of-the-science” understanding of emissions, transport and atmospheric chemistry. CTM
60 predictions provide more detailed composition information and full spatial coverage of air
61 pollution impacts with a typical temporal resolution of 1 hour. CTMs have great potential to fill
62 the time and space gaps in the central site monitoring dataset for PM measurements leading to
63 improved exposure assessment in epidemiological studies.

64
65 The CTM applications in epidemiology studies to date have generally used relatively
66 coarse spatial resolutions in order to reduce computational burden. Global CTMs have used
67 horizontal resolutions of over 100 km and regional CTMs have used resolution of 12-36 km.
68 These resolutions cannot capture fine spatial gradients of PM concentrations, especially in areas
69 with diverse topography and demography. Previous CTMs predictions used in epidemiology
70 studies have also been limited to time periods less than one year. Recently Zhang et al. (Zhang et

71 al., 2014a) evaluated the performance of the Community Multiscale Air Quality (CMAQ) model
72 over a 7-year period in the Eastern United States (U.S.), but no other long-term CTMs studies for
73 health effects analyses have been published to date. As a further limitation, previous
74 epidemiology studies based on CTM predictions have mostly used predicted particles with
75 aerodynamic diameter less than $2.5\mu\text{m}$ ($\text{PM}_{2.5}$) mass concentrations without taking full advantage
76 of the ability of CTMs to simultaneously estimate population exposure to multiple particle size
77 fractions, chemical components, and source contributions. The variation in CTM prediction bias
78 as a function of space and time due to uncertainties in model inputs (emissions, meteorological
79 fields, mechanism parameters) is often not sufficiently characterized to understand potential
80 impacts on health effects estimates. Detailed analyses are needed to assess the temporal and
81 spatial features of CTM predictions to identify accurate and/or unbiased information for
82 exposure assessment before such information can be applied in health effect studies (Beevers et
83 al., 2013).

84
85 The objective of the current study is to develop and apply advanced source-oriented
86 CTMs to predict the concentrations and sources for enhanced PM exposure assessment in
87 epidemiological studies over a long-term period with high spatial resolution in California.
88 California is chosen as the focus area for the current study because it has extensive infrastructure
89 to support CTM studies, and it has one of the largest populations in the U.S. that is experiencing
90 unhealthy levels of PM pollution. In 2013, 104 U.S. counties with a population of 65 million
91 people are in non-attainment with the National Ambient Air Quality Standards (NAAQS) for
92 $\text{PM}_{2.5}$ (EPA, 2013). Approximately half of that population (31 million people) lives in 29
93 California counties meaning that California suffers a disproportionately large share of U.S. PM-

94 related mortality (Fann et al., 2012). The California Air Resources Board (CARB) estimates that
95 14000 – 24000 California residents die prematurely each year due to particulate air pollution
96 (Tran, 2008). The severity of this problem has motivated extensive investments to support air
97 pollution studies. California has the densest ambient PM measurement network, accurate
98 emissions inventories, and the most health effects study groups of any state in the United States.
99 Rich datasets are available to support model application and evaluation.

100

101 The current study is the first attempt to address the sparse PM data problem in exposure
102 assessment using CTM results over a ~decadal time period (9 years from 2000 to 2008) over a
103 domain spanning ~1000 km at a spatial resolution of 4 km. Companion studies have modeled
104 primary PM_{2.5} and PM_{0.1} (particles with aerodynamic diameter less than 0.1µm) concentrations
105 and sources in California (Hu et al., 2014a; Hu et al., 2014b). The current paper, as the third in
106 the series, focuses on model evaluation of total (=primary+secondary) PM_{2.5} and major
107 components elemental carbon (EC), organic carbon (OC), nitrate, sulfate, ammonium),
108 emphasizing the aspects of temporal and spatial variations, to identify the features of the CTM
109 results that could add skill to the exposure assessment for epidemiological studies. A future study
110 will investigate the model capability for PM source apportionment of primary and secondary
111 organic aerosols, which is currently an area with great uncertainty.

112 **2. Methods**

113

114 **2.1 Air Quality Model Description**

115

116 The host air quality model employed in the current study is based on the Eulerian source-
117 oriented University of California-Davis/California Institute of Technology (UCD/CIT) chemical
118 transport model (Chen et al., 2010; Held, 2004; Held et al., 2005; Hixson et al., 2010; Hixson et
119 al., 2012; Hu et al., 2012; Hu et al., 2010; Kleeman and Cass, 2001; Kleeman et al., 1997;
120 Kleeman et al., 2007; Mahmud, 2010; Mysliwicz and Kleeman, 2002; Rasmussen et al., 2013;
121 Ying, 2008; Ying et al., 2007; Ying and Kleeman, 2006; Zhang and Ying, 2010). The UCD/CIT
122 model includes a complete description of atmospheric transport, deposition, chemical reaction,
123 and gas-particle transfer. The details of the standard algorithms used in the UCD/CIT family of
124 models have been described in the above references and therefore are not repeated here. Only the
125 aspects that are updated during the current study are discussed in the following section.

126
127 The photochemical mechanism used by the UCD/CIT model was updated to reflect the
128 latest information from smog-chamber experiments. The SAPRC-11 photochemical mechanism
129 (Carter and Heo, 2012a; Carter and Heo, 2013) was used to describe the gas-phase chemical
130 reactions in the atmosphere. The secondary organic aerosol (SOA) treatment was updated
131 following the method described in Carlton et al. (Carlton et al., 2010). Seven organic species
132 (isoprene, monoterpenes, sesquiterpenes, long-chain alkanes, high-yield aromatics, low-yield
133 aromatics, and benzene) are considered as precursors for SOA formation. A total of twelve semi-
134 volatile products and seven nonvolatile products are formed from the oxidation of the precursor
135 species. The gas-particle transfer of the semi-volatile and nonvolatile products in the UCD/CIT
136 model is dynamically calculated based on the gas vapor pressures calculated over the particle
137 surface and the kinetic limitations to mass transfer. The explicit chemical reactions and the
138 parameters for the thermodynamic equilibrium calculation (i.e., enthalpy of vaporization,

139 saturation concentrations, and stoichiometric yields) are provided in Carlton et al. and references
140 therein (Carlton et al., 2010).

141

142 Model simulations were configured using a one-way nesting technique with a parent
143 domain of 24 km horizontal resolution that covered the entire state of California (referred to as
144 CA_24km) and two nested domains with 4 km horizontal resolution that covered the Southern
145 California Air Basin (SoCAB) (referred to as SoCAB_4km) and San Francisco Bay Area + San
146 Joaquin Valley (SJV) + South Sacramento Valley air basins (referred to as SJV_4km) (shown in
147 Figure 1). The nested 4 km resolution domains are configured to cover the major ocean, coast,
148 urban, and rural regions that influence California's air quality and, most importantly, to cover
149 most of the California's population for the purpose of health effects analyses. Over 92% of
150 California's population lives in the 4 km domains based on the most recent census information.
151 The UCD/CIT model was configured with 16 vertical layers up to a height of 5 km above ground
152 level in all the mother and nested domains, with 10 layers in the first 1 km. Note that the use of
153 relatively shallow vertical domains is only appropriate in regions with well-defined air basins
154 and would not be appropriate for locations in the eastern U.S. or other regions with moderate
155 topography. Particulate composition, number and mass concentrations are represented in 15 size
156 bins, ranging from 0.01 to 10 μm in diameter. Primary particles are assumed to be internally
157 mixed, i.e., all particles within a size bin have the same composition. Previous studies (Ying et
158 al., 2007) have shown that this assumptions provides adequate predictions for total PM
159 concentrations relative to source-oriented mixing treatments in California when feedbacks to
160 meteorology are not considered (Zhang et al., 2014b).

161

2.2 Meteorology and Emissions

Hourly meteorology inputs (wind, temperature, humidity, precipitation, radiation, air density, and mixing layer height) were generated using the Weather Research and Forecasting model (WRF) v3.1.1 (Wei Wang, January 2010; William C. Skamarock, June 2008). Two-way nesting was used with the outer domain at 12 km resolution and the inner nested domain at 4 km resolution. North American Regional Reanalysis (NARR) data with 32 km resolution and 3-hour time resolution was used as initial and boundary conditions of the coarse 12 km domain. The WRF model was configured with 31 vertical layers up to 100 hPa (around 16 km). Four-dimensional data assimilation (FDDA) was used. The YSU boundary layer scheme, thermal diffusion land-surface scheme, and Monin-Obukhov surface layer scheme were used based on results from a previous study in California (Mahmud, 2010; Zhao et al., 2011). The surface wind was over-predicted with the original version of WRF, especially for wind speed less than 3 m/s, consistent with other studies in California (Angevine et al., 2012; Fast et al., 2014; Michelson et al., 2010a). Over-prediction of the slow winds caused under-prediction of concentrations during high pollution events. A recent study (Mass, C.F, personal communication) found that increasing the surface friction velocity (u^*) by 50% reduced the bias in surface wind predictions in a complex-terrain domain. This technique was tested and adopted in previous studies (Hu et al., 2012; Hu et al., 2014a; Mass and Ovens, 2010; Wang et al., 2015) where it improved the accuracy of air quality predictions. In the current study, a 1-year sensitivity simulation for California in the year of 2000 revealed that increasing u^* by 50% improved the mean wind bias from 1.15 m/s to -0.50 m/s, and lowered the root-mean-square error from 2.95 to 2.20 m/s (Hu et al., 2014a). It should be noted that this approach reduces positive bias for wind speeds less than

185 ~3 m/s, but increases negative bias at higher speeds. Analysis of the wind speed measurements
186 in California air basins shows that 78% of winds are less than 3 m/s. Therefore, increasing u^* by
187 50% in our study improves the wind predictions for a majority of cases during the modeling
188 period. Similar detailed evaluations should be conducted before applying the increased u^*
189 approach to other regions and periods. Hourly average meteorology outputs at the air quality
190 model vertical layer heights were created. The meteorology predictions were evaluated against
191 meteorological observations (CARB, 2011a). The meteorological statistical evaluation over the
192 period 2000-2006 has been presented in a previous study (Hu et al., 2014a), and the results in the
193 period 2007-2008 are consistent with those years. In summary, meteorology predictions of
194 temperature and wind speed generally meet benchmarks suggested by Emery et al. (2001). Mean
195 fractional biases (MFBs) of temperature and wind are generally within ± 0.15 , root mean square
196 errors (RMSEs) of temperature are around 4 °C, and RMSEs of wind are generally lower than 2.0
197 m/s, especially in the SoCAB and SJV air basins which are the focus of the current study.
198 Relative humidity is under-predicted, consistent with findings in other studies in California (Bao,
199 2008; Michelson et al., 2010b). Precipitation is also under-predicted with a MFB of -76.1% and
200 RMSE of 2.84 mm/hr. Wind, temperature and humidity are the major meteorological factors that
201 influence the PM concentrations. Further discussions of the uncertainties in meteorology
202 predictions on PM predictions are included in the Results section.

203

204 Hourly gridded gas and particulate emissions were generated using an updated version of
205 the emissions model described by Kleeman and Cass (Kleeman and Cass, 1998). The standard
206 emissions inventories from anthropogenic sources (i.e., point sources, stationary area sources,
207 and mobile sources) were provided by CARB. Size and composition resolved particle emissions

208 were specified using a library of primary particle source profiles measured during actual source
209 tests (Cooper, 1989; Harley et al., 1992; Hildemann et al., 1991a; Hildemann et al., 1991b;
210 Houck, 1989; Kleeman et al., 2008; Kleeman et al., 1999, 2000; Robert et al., 2007a; Robert et
211 al., 2007b; Schauer et al., 1999a, b, 2001, 2002a, b; Taback et al., 1979). A few studies have
212 revealed some uncertainties associated with the standard emissions inventories. Millstein and
213 Harley (Millstein and Harley, 2009) found that PM and NO_x emissions from diesel-powered
214 construction equipment were over-estimated by a factor of 3.1 and 4.5, respectively. Countess
215 (Countess, 2003) suggested that a scaling factor of 0.33 – 0.74 should be applied to the fugitive
216 dust emissions in the California's San Joaquin Valley. Therefore, scaling factors of 0.32 for off-
217 road diesel sources and 0.50 for dust emissions were applied in the current study. The EMFAC
218 2007 model (CARB, 2008) was used to scale the mobile emissions using predicted temperature
219 and relative humidity fields through the entire nine-year modeling episode. Biogenic emissions
220 were generated using the Biogenic Emissions Inventory System v3.14 (BEIS3.14), which
221 includes a 1-km resolution land cover database with 230 different vegetation types (Vukovich
222 and Pierce, 2002). Sea-salt emissions were generated on-line based on the formulation described
223 by de Leeuw et al. (de Leeuw et al., 2000) for the surf zone and the formulation described by
224 Gong (Gong, 2003) for the open ocean. Emissions from wildfires and open burning at 1 km × 1
225 km resolution were obtained from the Fire INventory from NCAR (FINN) (Hodzic et al., 2007;
226 Wiedinmyer et al., 2011). The FINN inventory provides SAPRC99 speciated daily emissions of
227 gaseous and particulate emissions (EC, organic matter (OM), PM_{2.5} and PM₁₀) based on satellite
228 observations of open burning events. Each open burning event is allocated to model grid cells of
229 each domain based on the reported longitude/latitude of the event and the area burned. The
230 emissions were injected at the height of the atmospheric mixing layer (PBL). The temporal

231 variation of wildfire emissions was obtained from the Western Regional Air Partnership
232 (WRAP) report (WRAP, 2005). A size distribution profile was calculated based on assumptions
233 described in Hodzic et al. (Hodzic et al., 2007).

234

235 **2.3 Ambient Air Quality Measurements**

236

237 The evaluation dataset was compiled from several measurement networks, including
238 CARB's "2011 Air Quality Data DVD" (CARB, 2011b) and the database maintained by the
239 Interagency Monitoring of Protected Visual Environments (IMPROVE). The data DVD includes
240 daily average mass concentrations of PM_{2.5}, EC, OC, nitrate, sulfate, ammonium, and trace
241 metals every 3 or 6 days at the sites of the PM_{2.5} Speciation Trends Network (STN) and the State
242 and Local Air Monitoring Stations (SLAMS). There are a total 13 PM_{2.5} speciation sites included
243 in the DVD covered in the 4 km domains during the modeling periods. The precision of STN
244 measurements is estimated to be 3.5%, 8.6%, and 3.9% for sulfate, nitrate, and ammonium,
245 respectively (Sickles Ii and Shadwick, 2002). Measured EC concentrations at 5 sites are found
246 to be exactly 0.5 µg/m³ on > 80% of the measurement days, suggesting corrupt or missing data
247 at these locations. Therefore these 5 sites were excluded in the evaluation for EC, but still
248 included in the evaluation for other PM components. The OC data were not blank corrected,
249 resulting in a positive artifact by the NIOSH5040 method that is equivalent to approximately 1
250 µg/m³. Measured OC concentrations were blank corrected in the current study by subtracting 1
251 µg/m³ from all OC measurements. The IMPROVE network provides daily average mass
252 concentrations every 3 days for PM_{2.5}, EC, OC, nitrate, sulfate, and soil. There are a total of 9
253 IMPROVE sites covered in the 4 km domains. The precision of IMPROVE measurements is

254 estimated to be 4–6% for PM_{2.5} mass, nitrate, and sulfate, and to be > 15% for EC and OC
255 ([http://vista.cira.colostate.edu/improve/Publications/OtherDocs/IMPROVEDataGuide/IMPROV
257 EDataGuide.htm](http://vista.cira.colostate.edu/improve/Publications/OtherDocs/IMPROVEDataGuide/IMPROV
256 EDataGuide.htm)). Daily average PM₁₀ mass measurements and hourly measurements of several
258 key gaseous pollutants (ozone, CO, NO, NO₂, and SO₂) are also included in the data DVD. There
259 are a total of 66 PM_{2.5} Federal Reference Method (FRM) sites covered in the 4 km domains.
260 Frank (Frank, 2006) found that FRM PM_{2.5} mass measured using STN monitors was within ±
261 30% of reconstructed fine mass (RCFM) concentrations measured using IMPROVE monitors.

261 **3. Results and Discussion**

262 **3.1 Statistical evaluation**

263

264 Statistical measures of MFB and mean fractional error (MFE) were calculated to evaluate
265 the accuracy of model estimates in space and time. Boylan and Russell (Boylan and Russell,
266 2006) proposed concentration dependent MFB and MFE performance goals and criteria,
267 realizing that lower concentrations are more difficult to accurately predict. The performance
268 goals are the level of accuracy close to the best that a model can be expected to achieve, while
269 performance criteria are the level of accuracy acceptable for standard modeling applications.

270

271 Figures 2 and 3 show the monthly MFB and MFE values, respectively, of predicted daily
272 average EC, OC, nitrate, ammonium, sulfate and total PM_{2.5} mass in the 4 km domains.
273 Measured EC, OC, nitrate, ammonium, and total PM_{2.5} mass concentrations follow similar
274 seasonal patterns with high concentrations occurring in winters (indicated by blue colors in
275 figures) and low concentrations occurring in summers (indicated by red colors in figures). These
276 patterns are driven by the meteorological cycles (i.e., lower mixing layer and wind speed

277 providing less dilution, and lower temperature encouraging partitioning of ammonium nitrate to
278 the particle phase) and the emissions variations (i.e., additional wood burning emissions for
279 home heating in winters). The opposite seasonal variations in sulfate concentrations are
280 observed, due to higher oxidation rates from S(IV) to S(VI) and higher sulfur emissions from
281 natural sources in summer (Bates et al., 1992).

282

283 EC predictions are in excellent agreement with measurements. MFBs in all months and
284 MFEs in 107 months out of the total 108 months are within the model performance goal. EC
285 MFBs and MFEs show no significant difference among months/seasons, indicating consistently
286 good EC performance during the entire 9-year modeling period. OC, nitrate, sulfate, and
287 ammonium, the PM components that include the secondary formation pathways, meet the MFBs
288 model performance criteria in 71%, 73%, 46%, and 92% of the simulated months, respectively.
289 These components generally have good agreement between predictions and measurements in
290 winter months, with only a few months not meeting the performance criteria. When analyzing by
291 season, predicted concentrations of these species are found to be more biased in summer months,
292 especially for sulfate and nitrate. Different factors influence the seasonal profile of each species.
293 The more significant OC under-prediction in summertime is mainly associated with the under-
294 prediction of SOA due to incomplete knowledge of SOA formation mechanism at the present
295 time. Similar patterns have been reported in other modeling studies outside California (Matsui et
296 al., 2009; Volkamer et al., 2006; Zhang et al., 2014a; Zhang and Ying, 2011). Measured nitrate
297 concentrations in summertime ($1-5 \mu\text{g}/\text{m}^3$) are factors of 2-5 lower than concentrations in
298 wintertime ($5-12 \mu\text{g}/\text{m}^3$). Model predictions tend to underestimate the low particle phase nitrate
299 concentrations in summer, especially when temperatures exceed 25°C . Model predictions for

300 particulate nitrate are usually less than $1 \mu\text{g}/\text{m}^3$ under these conditions, while $2\text{-}3 \mu\text{g}/\text{m}^3$ nitrate
301 concentrations are still observed in the ambient air. Similar under-predictions of summertime
302 nitrate have been reported in other regional modeling studies (Appel et al., 2008; Tesche et al.,
303 2006; Yu et al., 2005; Zhang et al., 2014a). Model calculations reflect thermodynamics and
304 kinetic gas-particle transfer for ammonium nitrate in mixed particles, suggesting that some other
305 form of nitrate is present in the real atmosphere, such as organo-nitrates (Day et al., 2010).
306 Sulfate concentrations are consistently under-predicted throughout the modeling period at all
307 locations, especially in southern California where the measured sulfate concentrations are
308 highest. Under-prediction of sulfate has also been reported by other regional modeling studies in
309 California (Chen et al., 2014; Fast et al., 2014), using different air quality models (e.g., CMAQ,
310 WRF-Chem). This consistent behavior suggests that the specific model is not the cause of the
311 sulfate under-prediction. A global model study that included ocean DMS emissions showed a
312 better sulfate performance in California (Walker et al., 2012). Therefore, missing emissions
313 sources such as the sulfur emitted as dimethyl sulfide (DMS) from the Pacific Ocean likely
314 contribute to the sulfate under-predictions in the current study. The sulfate concentrations at the
315 sites in southern California are ~ 2 to 3 times higher than in northern California, and are under-
316 predicted by an even larger amount (with MFBs around -1.0). It is therefore likely that
317 anthropogenic sulfur sources are missing in southern California in addition to background DMS
318 sources. In the remote areas where the sulfate concentrations are low, the omission of nucleation
319 processes in the current study could reduce seed aerosol surface area onto which sulfuric acid
320 can condense. This factor could contribute to the under-prediction of sulfate mass in these
321 regions along with the missing sulfur sources. Ammonium is drawn to acidic particles and so

322 ammonium concentration predictions reflect the combined trends of nitrate and sulfate
323 predictions.

324

325 The model predictions of total PM_{2.5} mass, as a summation of all components, show very
326 good agreement with measurements, with only 3 summer months and 2 spring months (5% of all
327 simulated months) not meeting the performance criteria, and 78% and 75% of months within the
328 performance goals for MFB and MFE, respectively. The largest biases in the total PM_{2.5} mass
329 occur in summer. Under-prediction in summer sulfate and OC contribute to negative biases in
330 the total PM_{2.5} mass predictions. Sulfate and OC concentrations in summer accounted for ~18%
331 and ~37% of the total PM_{2.5} mass. Sulfate and OC under-prediction contributed to a combined
332 ~37% under-prediction of total PM_{2.5} mass. However, positive biases in predicted dust
333 concentrations rich in crustal elements such as aluminum and silica (Hu et al., 2014a)
334 compensate for the under-predictions in carbonaceous components and water-soluble ions
335 described above.

336

337 Figure 4 shows the MFB and MFE values of particulate species of PM_{2.5} total mass, EC,
338 OC, nitrate, sulfate, ammonium and gaseous species of O₃, CO, NO, NO₂, SO₂ using daily
339 averages across all measurement sites during the entire modeled 9-year period. PM_{2.5} total mass,
340 EC, OC, ammonium and gaseous species of O₃, CO, NO₂ have MFBs within ±0.3 and MFE less
341 than 0.75, indicating general agreement between predictions and measurement for these species.
342 Nitrate and NO have MFBs of -0.4 and -0.28, respectively, but MFEs of 0.8 and 1.07,
343 respectively. The relatively moderate or small bias combined with relatively large error indicates
344 that the daily predictions miss the extremely high and low concentrations. Sulfate and SO₂ have

345 high MFBs of -0.7 and -0.5, respectively, and high MFEs of 0.8 and 0.9, respectively, indicating
346 that these species are consistently under-predicted.

347
348 Concentrations averaged over longer times, such as 1 month or 1 year, are used in some
349 air pollution-health effects studies. A previous examination of primary particles in California
350 revealed that air quality model predictions are more accurate over longer averaging time because
351 the influence of extreme events and short-term variability is reduced as the averaging period gets
352 longer (Hu et al., 2014a). Figure 4 compares the MFB and MFE values for total
353 (=primary+secondary) particulate matter and gaseous species using daily, monthly, and annual
354 averages across all sites in the 4 km domains. The results demonstrate that longer averaging
355 times produce better agreement between model predictions and measurements (except for
356 sulfate, which is under-predicted due to missing emissions) because they remove the effects of
357 random measurement errors at monitoring stations and variations in actual emissions rates that
358 are not reflected in seasonally-averaged emissions inventories. The reduced errors associated
359 with longer averaging times indicate that model results may be most useful in epidemiological
360 studies that can take advantage of averaging times ≥ 1 month.

361 **3.2 Spatial and temporal variations**

362
363 Figure 5 panel (a) shows the predicted and measured monthly average concentrations of
364 1-h peak O₃ at 5 major urban sites (Sacramento, Fresno, Bakersfield, Los Angeles, and
365 Riverside). Strong seasonal variations are observed in measured and predicted 1-h peak O₃. The
366 measured 1-h peak O₃ shows seasonal variation from 100 ppb in summertime to 20 ppb in
367 wintertime. The predicted high 1-h peak O₃ concentrations in non-winter months are in good

368 agreement with, or slightly higher than, ambient measured concentrations at all sites. This is
369 consistent with studies in the eastern U.S. (Zhang et al., 2014a), which found similar slight over-
370 predictions of summer O₃ concentrations. Predicted 1-h peak O₃ concentrations in cold winter
371 months, however, are generally higher than measured values. Photochemical reaction rates in
372 wintertime months are slow and the predicted O₃ concentration at the surface mostly reflects
373 downward mixing of the aloft background O₃ followed by titration by surface NO emissions.
374 The STN measurement sites in California are located in urban areas that are close to major
375 freeways (see the site locations and nearby sources information in (Hu et al., 2014a)). The 4 km
376 × 4 km model grid cells that contain both freeways and monitors dilute the high NO
377 concentrations around the measurement sites leading to an under-prediction of O₃ titration and an
378 over-prediction of O₃ concentrations. EPA recommends a threshold O₃ value of 60 ppb for
379 model O₃ evaluations (U.S.EPA, 2007), which means that wintertime O₃ concentrations at the
380 urban sites will generally not be considered in the formal model evaluation.

381

382 Figure 5 panels (b) and (c) show the predicted and measured monthly average CO and
383 NO concentrations. Strong seasonal variations in CO and NO can be observed, with wintertime
384 concentrations that are a factor of 3-5 higher than summertime concentrations. Model predictions
385 generally reproduce the seasonal variations except at the Riverside site where predicted seasonal
386 variations are weaker than measurements. The model performance varies by simulation year and
387 location. At the Sacramento and Fresno sites, predicted CO is in good agreement with measured
388 concentrations in all months of 2002 through 2006, but CO is under-predicted in winter months
389 of 2000-2001 and slightly over-predicted in most months of 2007-2008. At the Bakersfield site,
390 CO is under-predicted in 2000-2003 and in good agreement with measurements in 2004-2005

391 (after which further measurements are not available). At the Los Angeles site, CO is in good
392 agreement in 2000-2003, and over-predicted in the later years. At the Riverside site, CO is
393 under-predicted in all months of 2000-2003, under-predicted in non-summer months in 2004-
394 2006, and in general agreement with measurements in 2007-2008. NO predictions generally
395 agree well with measured NO concentrations in 2000-2004 at Sacramento, Fresno, Bakersfield
396 and Los Angeles, and then are over-predicted in the later years. NO at Riverside is under-
397 predicted in the winter months of 2000-2003, and over-predicted in the summer months of 2004-
398 2008. Mobile emissions are the dominant sources of CO and NO in California, contributing >
399 80% of total anthropogenic emissions (CARB, 2012). The results of the current modeling study
400 suggest that uncertainties in the mobile emissions exist both in time and space.

401

402 A clear and similar decreasing trend is apparent in measured CO and NO concentrations
403 from 2000-2008. This inter-annual trend is not well captured by the model predictions due to the
404 uncertainties in the emissions. An adjusted NO prediction (NO_adj) can be calculated using CO
405 as a tracer for the mobile emissions and dilution according to the equation:

$$406 \quad \text{NO}_{\text{adj}} = \text{NO}_{\text{noadj}} * \text{CO}_{\text{predicted}} / \text{CO}_{\text{measured}}$$

407 where NO_noadj is the NO predictions before the adjustment (i.e., the concentrations showing in
408 Figure 5(c)). NO_adj has higher correlation coefficient (R^2) with measured NO concentrations
409 than the NO_noadj prediction at all the five monitoring sites (as shown in Figure 7) and NO_adj
410 has a regression slope closer to 1.0 than NO_noadj at 3 out of 5 sites. This suggests that either
411 emissions or physical dilution processes in the model contribute to the errors observed in Figure
412 5 (in addition to the possibility of errors in model chemistry). Unfortunately, the large variation
413 in the correction factor among different locations suggests that these scaling factors cannot be

414 simply interpolated/extrapolated from the indicated five monitoring sites to the full modeling
415 domain.

416

417 Figure 5 panels (d) and Figure 6 (a) show the predicted and measured monthly average
418 ammonium and nitrate concentrations. Ammonium nitrate is a major $PM_{2.5}$ component in
419 California, especially in wintertime when the low temperature and high relative humidity favor
420 partitioning to the condensed phase. The monthly average ammonium and nitrate results
421 demonstrate similar model performance. The predicted concentrations agree reasonably well
422 with measured ambient concentrations and seasonal variations. Model predictions are lower than
423 measured values in the early years, especially during winter months when concentrations are
424 highest. This pattern is very consistent with CO model performance, suggesting mobile
425 emissions are under-estimated for the early years of the simulation period. Nitrate is formed
426 through NO oxidation to nitric acid but NO concentrations are not under-predicted, suggesting
427 that the chemical conversion of NO to nitric acid is too slow. Carter and Heo (Carter and Heo,
428 2012b) suggested that SAPRC11 mechanism systematically under-predicts OH radical
429 concentrations by ~30%, which would be consistent with the observed trends.

430

431 Gas-particle partitioning of ammonium nitrate depends on temperature and relative
432 humidity. While there is no systematic bias in WRF temperature, relative humidity is generally
433 under-predicted by up to 40% over California. A one-year sensitivity analysis was conducted
434 with RH increased uniformly by +30% (but not to exceed 95%, and all other meteorological
435 parameters were kept the same) in 2008 to investigate the impact of the relative humidity bias on
436 particulate nitrate predictions. The arbitrary increase in RH by 30% in the air quality model

437 simulations yields an upper bound estimate of the nitrate sensitivity to RH. Figure 8 compares
438 the monthly average nitrate concentrations predicted with the original RH (denoted as “RH_ori”
439 case) and the enhanced RH (denoted as “RH+0.3” case) at Sacramento and Fresno. Nitrate
440 predictions are generally higher in the “RH+0.3” case due to more particle phase water available
441 to absorb nitrate into the condensed phase. The nitrate predictions at Sacramento are significantly
442 improved during most months in 2008, suggesting this area suffers from the low RH bias in the
443 WRF predictions. Nitrate at Fresno is improved mostly in the winter and spring, but is still
444 under-predicted during the time period with peak winter concentrations, indicating this area is
445 influenced by other factors besides RH. Nitrate predictions at Fresno in summer and fall are
446 lower when RH is enhanced, due to faster deposition caused by larger particle sizes with more
447 particle phase water. The uniform RH increase of 0.3 in this region is likely unrealistically large
448 during these months.

449

450 Figure 6 panel (b) shows the OC predictions and measurements. Organic aerosol in
451 California it is typically the second most abundant species, after ammonium nitrate. In the
452 comparison, an OM/OC ratio of 1.6 (Turpin and Lim, 2010) is applied to convert primary
453 organic aerosol OM back to OC for comparison to measured concentrations. The conversion
454 ratios for SOA species are taken from Table 1 in Carlton et al. (Carlton et al., 2010). Predicted
455 OC agrees reasonably well with measured concentrations, but is lower than the wintertime high
456 concentrations in the early years, similar to other PM components. Predicted OC in summers is
457 also in good agreement with measurements at the indicated monitoring sites. As mentioned
458 previously, these sites are all near major freeways and therefore OC is dominated by primary
459 organic aerosols. Larger bias is found at sites distant from local sources where SOA becomes

460 more important. More analysis about the concentrations and sources of the OC results are
461 included in a companion paper (Hu, Manuscript in preparation).

462

463 Figure 6 panel (c) shows that predicted EC concentrations agree well with measured
464 concentrations. High measured EC concentrations in a few winter months in the early years are
465 under-predicted, but EC concentrations in the summer months are generally over-predicted.

466

467 Figure 6 panel (d) shows that monthly average predictions for $PM_{2.5}$ mass concentrations
468 agree well with observations, and seasonal trends are generally captured with high
469 concentrations in winter, and low concentrations in summer. $PM_{2.5}$ is over-predicted in summer
470 months when nitrate, sulfate, and ammonium are found to be under-predicted. These trends
471 reflect the over-prediction of the primary components, mostly dust particles, in the model
472 calculations (Hu et al., 2014a). This result suggests that a uniform scaling factor of 0.5 for dust
473 emissions may not be appropriate. A smaller factor (for example, a factor of 0.25 was used in
474 the eastern U.S. (Tesche et al., 2006)) or a spatially resolved method that accounts for the land-
475 use types (Pace, 2005) should be used for future studies in California.

476

477 California experiences the highest $PM_{2.5}$ concentrations in wintertime, caused by stagnant
478 meteorological conditions characterized by low wind speed and shallow atmospheric mixing
479 layer. The WRF model tends to over-predict wind speed during low wind speed events (≤ 2 m/s)
480 in California (Zhao et al., 2011). Increasing u^* by 50% improves the WRF wind prediction but
481 still over-predicts wind speed during events when measured wind speed is <1.5 m/s. A zero-
482 order approximation of air pollutant concentration (Mahmud, 2010) is:

483
$$C = \frac{E}{V} = \frac{E}{u \times H} \quad (1)$$

484 where C is the pollutant concentration, E is the source pollutant emission rate, V is the air
485 ventilation rate which is equal to (wind speed \times mixing height), u and H are the horizontal wind
486 speed and mixing height, respectively. The concentration is linearly dependent on the inverse
487 wind speed ($1/u$). Figure 9 shows the MFBs of the predicted atmospheric inverse wind speed
488 ($1/u$) as a function of the observed atmospheric inverse wind speed. Also shown in Figure 9 are
489 the MFBs of PM component concentrations as a function of the observed concentrations. The
490 MFBs decrease when the inverse wind speed or concentrations increase, indicating low inverse
491 wind speed/concentrations are over-predicted, but high inverse wind speed /concentrations are
492 under-predicted. The trends of inverse wind speed and concentrations are well correlated,
493 indicating that simple wind bias leads to bias in PM predictions, especially during the events
494 with high PM pollution. The correlation with $1/u$ MFB is stronger for primary PM component(s)
495 than for secondary components, indicating that additional processes affect the secondary PM,
496 such as chemistry, gas-particle partitioning, etc. Sulfate bias has the weakest correlation to
497 inverse ventilation bias, because sulfate bias is mainly driven by the bias in sulfur emissions.

498

499 Figure 10 shows the predicted 9-year average concentrations of $PM_{2.5}$, EC, OC, nitrate,
500 sulfate, and ammonium, compared with measured average concentrations over California. High
501 concentrations of all PM pollutants occur in the urban areas with large population, indicating that
502 most of the PM is generated by anthropogenic activities. The predicted spatial distributions
503 generally agree well with measurements, but provide much more detailed information. $PM_{2.5}$
504 concentrations are over-predicted in the SJV air basin due to an over-prediction of agricultural
505 dust. High OC concentrations were measured at two sites in northern California due to intense

506 wood burning. The two sites are in the 24 km model domain but outside the 4 km, therefore the
507 predicted OC concentrations in the 24 km grids do not agree well with the measurements at this
508 location. This finding confirms that 24 km resolution is probably too coarse for health effects
509 studies and justifies the use of 4 km grids over the majority of California's population in the
510 current work. Background sulfate concentrations at IMPOVE sites were measured to be 0.6-1
511 $\mu\text{g}/\text{m}^3$ but higher concentrations of 2~3 $\mu\text{g}/\text{m}^3$ were measured in Southern California. Model
512 calculations do not reproduce this concentration enhancement, leading to an under-prediction in
513 the concentrations of this $\text{PM}_{2.5}$ species.

514 **3.3 Discussion**

515
516 In general, the reasonable agreement between model predictions and measurement builds
517 confidence that the model predictions can provide a reasonable estimate of exposure fields in
518 locations with no available measurements. The detailed analysis described in the previous
519 section identifies several aspects that must be considered when applying the data in the health
520 effect studies. For the gaseous pollutants, daily maximum O_3 predictions are in good agreement
521 with measurements across the entire modeling domain. Seasonal and annual variations are
522 captured accurately. Therefore daily maximum O_3 predictions can be used in health analyses
523 with high confidence. The predictions also capture the seasonal variations in NO and CO, but do
524 not reflect the long-term trends, especially in southern California. Predicted monthly averages of
525 NO and CO in northern California are preferred over daily averages for use in health analyses.
526 For the PM pollutants, daily concentrations and spatial distributions of EC and total $\text{PM}_{2.5}$ mass
527 generally agree well with observations, but monthly averages should be considered first in health
528 studies as they are in better agreement with observations than shorter averages. Predicted OC in

529 winter is also reasonably accurate, but OC in summer should be used with caution. Sulfate and
530 nitrate are both under-predicted. Sulfate has greater bias in southern California than in northern
531 California, while nitrate has consistent bias throughout the modeling domain. This suggests that
532 the spatial distribution information of nitrate might still be useful for health effect studies that
533 use contrasts in exposure as a function of location, but sulfate data are likely not useful in health
534 effects studies at the present time.

535

536 Predicted monthly averages for PM concentrations are more accurate than daily averages,
537 suggesting that the PM exposure predictions will be most useful in studies that can take
538 advantage of averaging times ≥ 30 days. Longer averaging times smooth out short-term PM
539 variations that could be useful in some epidemiological studies that focus on short term changes
540 in health effects. To get more accurate pollutant predictions at shorter timescales would require
541 more accurate representation of emissions, meteorological conditions, and atmospheric
542 chemistry at these time scales. Many intensive studies that manually corrected input data have
543 focused on high temporal resolution for short periods (generally less than 1 month), such as the
544 California Regional PM₁₀/PM_{2.5} Air Quality Study (CRPAQS) (Ying, 2008). It is currently
545 impractical to carry out such efforts for a ~10 year modeling period in which there are a large
546 number of special events that are not represented by automated meteorology and emissions
547 models. The atmospheric modeling community continues to refine tools that can capture and
548 accurately represent these special cases. For example, the current study includes automatic
549 detection and incorporation of wildfire emissions into the modeling system based on satellite
550 observations. This automated feature was not generally available in previous studies. Future
551 advances will detect transportation patterns responding to traffic accidents or holiday traffic

552 jams, drought effects on biogenic emissions, etc. These future advances will improve models to
553 have more accurate predictions in both short- (<1 month) and long- (> 1 month) averaging times.

554 **4. Conclusions**

555 For the first time, a ~decadal (9 year) CTM air quality model simulation with 4 km
556 horizontal resolution over populated regions has been conducted in California to provide air
557 quality data for health effects studies. Model predictions are compared to measurements in order
558 to evaluate both the spatial and temporal accuracy of the results. The performance of the source-
559 oriented UCD/CIT air quality model is satisfactory for O₃, PM_{2.5}, and EC (both spatially and
560 temporally). Predicted OC, nitrate, and ammonium are less satisfactory, but generally meet
561 standard model performance criteria. OC bias is larger in summertime than wintertime mainly
562 due to an incomplete understanding of SOA formation mechanisms. Bias in predicted
563 ammonium nitrate is associated with uncertainties in emissions, the WRF predicted relative
564 humidity fields, and the chemistry mechanism. Predicted sulfate is not satisfactory due to
565 missing sulfur sources in the emissions. The CO and NO (species dominated by mobile
566 emissions) results reveal significant temporal and spatial uncertainties associated with the mobile
567 emissions generated by the EMFAC 2007 model. The WRF model tends to over-predict wind
568 speed during stagnation events, leading to under-predictions of high PM concentrations, usually
569 in winter months. The WRF model also generally under-predicts relative humidity, resulting in
570 less particulate nitrate formation especially during winter months. Despite the issues noted
571 above, predicted spatial distributions of PM components are in reasonably good agreement with
572 measurements. Predicted seasonal and annual variations also generally agree well with
573 measurements. Better model performance with longer averaging time is found in the predictions,
574 suggesting that model results with averaging times ≥ 1 month should be first considered in

575 epidemiological studies. All model results included in the current manuscript can be
576 downloaded free of charge at <http://faculty.engineering.ucdavis.edu/kleeman/>.

577 **Acknowledgement**

578
579 This study was funded by the United States Environmental Protection Agency under Grant No.
580 83386401. Although the research described in the article has been funded by the United States
581 Environmental Protection Agency it has not been subject to the Agency's required peer and
582 policy review and therefore does not necessarily reflect the reviews of the Agency and no official
583 endorsement should be inferred.

584 **References**

- 585
586 Anenberg, S.C., Horowitz, L.W., Tong, D.Q., West, J.J., 2010. An Estimate of the Global
587 Burden of Anthropogenic Ozone and Fine Particulate Matter on Premature Human Mortality
588 Using Atmospheric Modeling. *Environmental Health Perspectives* 118, 1189-1195.
589 Angevine, W.M., Eddington, L., Durkee, K., Fairall, C., Bianco, L., Brioude, J., 2012.
590 Meteorological Model Evaluation for CalNex 2010. *Monthly Weather Review* 140, 3885-3906.
591 Appel, K.W., Bhave, P.V., Gilliland, A.B., Sarwar, G., Roselle, S.J., 2008. Evaluation of the
592 community multiscale air quality (CMAQ) model version 4.5: Sensitivities impacting model
593 performance; Part II - particulate matter. *Atmospheric Environment* 42, 6057-6066.
594 Bao, J.W., Michelson, S. A., Persson, P. O. G., Djalalova, I. V., Wilczak, J. M., 2008. Observed
595 and WRF-simulated low-level winds in a high-ozone episode during the Central California
596 Ozone Study. *Journal of Applied Meteorology and Climatology* 47, 2372-2394.
597 Barnett, A.G., Plonka, K., Seow, W.K., Wilson, L.A., Hansen, C., 2011. Increased traffic
598 exposure and negative birth outcomes: a prospective cohort in Australia. *Environmental health*
599 10, 26.
600 Bates, T.S., Lamb, B.K., Guenther, A., Dignon, J., Stoiber, R.E., 1992. Sulfur emissions to the
601 atmosphere from natural sources. *J Atmos Chem* 14, 315-337.
602 Beelen, R., Hoek, G., van den Brandt, P.A., Goldbohm, R.A., Fischer, P., Schouten, L.J.,
603 Armstrong, B., Brunekreef, B., 2008. Long-term exposure to traffic-related air pollution and lung
604 cancer risk. *Epidemiology* 19, 702-710.
605 Beeson, W.L., Abbey, D.E., Knutsen, S.F., 1998. Long-term concentrations of ambient air
606 pollutants and incident lung cancer in California adults: Results from the AHSMOG study.
607 *Environmental Health Perspectives* 106, 813-822.
608 Beevers, S.D., Kitwiroon, N., Williams, M.L., Kelly, F.J., Ross Anderson, H., Carslaw, D.C.,
609 2013. Air pollution dispersion models for human exposure predictions in London. *J Expos Sci*
610 *Environ Epidemiol* 23, 647-653.

611 Bell, M.L., Belanger, K., Ebisu, K., Gent, J.F., Lee, H.J., Koutrakis, P., Leaderer, B.P., 2010.
612 Prenatal exposure to fine particulate matter and birth weight: variations by particulate
613 constituents and sources. *Epidemiology* 21, 884-891.

614 Bell, M.L., Dominici, F., Ebisu, K., Zeger, S.L., Samet, J.M., 2007. Spatial and temporal
615 variation in PM(2.5) chemical composition in the United States for health effects studies.
616 *Environ Health Perspect* 115, 989-995.

617 Boylan, J.W., Russell, A.G., 2006. PM and light extinction model performance metrics, goals,
618 and criteria for three-dimensional air quality models. *Atmospheric Environment* 40, 4946-4959.

619 Brauer, M., Lencar, C., Tamburic, L., Koehoorn, M., Demers, P., Karr, C., 2008. A cohort study
620 of traffic-related air pollution impacts on birth outcomes. *Environ Health Perspect* 116, 680-686.

621 Bravo, M.A., Fuentes, M., Zhang, Y., Burr, M.J., Bell, M.L., 2012. Comparison of exposure
622 estimation methods for air pollutants: Ambient monitoring data and regional air quality
623 simulation. *Environmental research* 116, 1-10.

624 Burnett, R.T., Brook, J., Dann, T., Delocla, C., Philips, O., Cakmak, S., Vincent, R., Goldberg,
625 M.S., Krewski, D., 2000. Association between particulate- and gas-phase components of urban
626 air pollution and daily mortality in eight Canadian cities. *Inhalation Toxicology* 12, 15-39.

627 Cao, J.J., Xu, H.M., Xu, Q., Chen, B.H., Kan, H.D., 2012. Fine Particulate Matter Constituents
628 and Cardiopulmonary Mortality in a Heavily Polluted Chinese City. *Environmental Health*
629 *Perspectives* 120, 373-378.

630 CARB, 2008. Calculating emission inventories for vehicles in California. User's Guide EMFAC
631 2007 version 2.30 Accessed in 2010.

632 CARB, 2011a. Meteorology Data Query Tool (PST),
633 <http://www.arb.ca.gov/aqmis2/metsselect.php>. Accessed in 2011.

634 CARB, 2012. Almanac Emission Projection Data (published in 2009),
635 <http://www.arb.ca.gov/app/emsinv/emssumcat.php>. Accessed in 2012.

636 CARB, 2011b. Database: California Air Quality Data - Selected Data Available for Download
637 <<http://www.arb.ca.gov/aqd/aqcdcd/aqcdcdld.htm>>. Accessed in 2011.

638 Carlton, A.G., Bhave, P.V., Napelenok, S.L., Edney, E.D., Sarwar, G., Pinder, R.W., Pouliot,
639 G.A., Houyoux, M., 2010. Model Representation of Secondary Organic Aerosol in CMAQv4.7.
640 *Environmental Science & Technology* 44, 8553-8560.

641 Carter, W.P.L., Heo, G., 2012a. DEVELOPMENT OF REVISED SAPRC AROMATICS
642 MECHANISMS. Final Report to California Air Resources Board Contracts No. 07-730 and 08-
643 326.

644 Carter, W.P.L., Heo, G., 2012b. DEVELOPMENT OF REVISED SAPRC AROMATICS
645 MECHANISMS. Report to the California Air Resources Board, Contract No. 07-730 and 08-326

646 Carter, W.P.L., Heo, G., 2013. Development of revised SAPRC aromatics mechanisms.
647 *Atmospheric Environment* 77, 404-414.

648 Chen, J., Lu, J., Avise, J.C., DaMassa, J.A., Kleeman, M.J., Kaduwela, A.P., 2014. Seasonal
649 modeling of PM2.5 in California's San Joaquin Valley. *Atmospheric Environment* 92, 182-190.

650 Chen, J.J., Ying, Q., Kleeman, M.J., 2010. Source apportionment of wintertime secondary
651 organic aerosol during the California regional PM(10)/PM(2.5) air quality study. *Atmospheric*
652 *Environment* 44, 1331-1340.

653 Chen, Y.Y., Ebenstein, A., Greenstone, M., Li, H.B., 2013. Evidence on the impact of sustained
654 exposure to air pollution on life expectancy from China's Huai River policy. *P Natl Acad Sci*
655 *USA* 110, 12936-12941.

656 Cooper, J.A.e.a., 1989. Dinal Appendix V-G, PM10 source composition library for the South
657 Coast Air Basin. Technical Report, South Coast Air Quality Management District, Diamond Bar,
658 California.

659 Correia, A.W., Pope, C.A., Dockery, D.W., Wang, Y., Ezzati, M., Dominici, F., 2013. Effect of
660 Air Pollution Control on Life Expectancy in the United States An Analysis of 545 US Counties
661 for the Period from 2000 to 2007. *Epidemiology* 24, 23-31.

662 Countess, R.J., 2003. Reconciling Fugitive Dust Emission Inventories with Ambient
663 Measurements. 12th Annual EPA Emission Inventory Conference San Diego, CA.

664 Day, D.A., Liu, S., Russell, L.M., Ziemann, P.J., 2010. Organonitrate group concentrations in
665 submicron particles with high nitrate and organic fractions in coastal southern California.
666 *Atmospheric Environment* 44, 1970-1979.

667 de Leeuw, G., Neele, F.P., Hill, M., Smith, M.H., Vignali, E., 2000. Production of sea spray
668 aerosol in the surf zone. *Journal of Geophysical Research-Atmospheres* 105, 29397-29409.

669 Dockery, D.W., 2001. Epidemiologic evidence of cardiovascular effects of particulate air
670 pollution. *Environmental Health Perspectives* 109, 483-486.

671 Dockery, D.W., Pope, C.A., Xu, X.P., Spengler, J.D., Ware, J.H., Fay, M.E., Ferris, B.G.,
672 Speizer, F.E., 1993. An Association between Air-Pollution and Mortality in 6 United-States
673 Cities. *New England Journal of Medicine* 329, 1753-1759.

674 Emery, C., Tai, E., Yarwood, G., 2001. Enhanced meteorological modeling and performance
675 evaluation for two texas episodes, in: Report to the Texas Natural Resources Conservation
676 Commission, p.b.E., Internatioanl Corp (Ed.), Novato, CA.

677 EPA, U.S., 2013. Particulate Matter (PM2.5) Area Information (2006 Standard).
678 <http://www.epa.gov/airquality/greenbook/rindex.html> Accessed in January 2014.

679 Fann, N., Lamson, A.D., Anenberg, S.C., Wesson, K., Risley, D., Hubbell, B.J., 2012.
680 Estimating the National Public Health Burden Associated with Exposure to Ambient PM2.5 and
681 Ozone. *Risk Anal* 32, 81-95.

682 Fast, J.D., Allan, J., Bahreini, R., Craven, J., Emmons, L., Ferrare, R., Hayes, P.L., Hodzic, A.,
683 Holloway, J., Hostetler, C., Jimenez, J.L., Jonsson, H., Liu, S., Liu, Y., Metcalf, A.,
684 Middlebrook, A., Nowak, J., Pekour, M., Perring, A., Russell, L., Sedlacek, A., Seinfeld, J.,
685 Setyan, A., Shilling, J., Shrivastava, M., Springston, S., Song, C., Subramanian, R., Taylor, J.W.,
686 Vinoj, V., Yang, Q., Zaveri, R.A., Zhang, Q., 2014. Modeling regional aerosol and aerosol
687 precursor variability over California and its sensitivity to emissions and long-range transport
688 during the 2010 CalNex and CARES campaigns. *Atmos. Chem. Phys.* 14, 10013-10060.

689 Ford, I., Li, X.Y., Donaldson, K., MacNee, W., Seaton, A., Greaves, M., 1998. Particulate air
690 pollution and cardiovascular risk: Increased factor VIIc follows exposure to ultrafine particles.
691 *Brit J Haematol* 101, 80-80.

692 Franchini, M., Mannucci, P.M., 2009. Particulate Air Pollution and Cardiovascular Risk: Short-
693 term and Long-term Effects. *Semin Thromb Hemost* 35, 665-670.

694 Frank, N.H., 2006. Retained nitrate, hydrated sulfates, and carbonaceous mass in Federal
695 Reference Method fine particulate matter for six eastern US cities. *Journal of the Air & Waste*
696 *Management Association* 56, 500-511.

697 Franklin, M., Koutrakis, P., Schwartz, J., 2008. The role of particle composition on the
698 association between PM2.5 and mortality. *Epidemiology* 19, 680-689.

699 Franklin, M., Zeka, A., Schwartz, J., 2007. Association between PM2.5 and all-cause and
700 specific-cause mortality in 27 US communities. *Journal of Exposure Science and Environmental*
701 *Epidemiology* 17, 279-287.

702 Goldgewicht, C., 2007. Association between surrounding air pollution and daily mortality in
703 subjects with diabetes and cardiovascular complications. *Environnement Risques & Sante* 6, 15-
704 16.

705 Gong, S.L., 2003. A parameterization of sea-salt aerosol source function for sub- and super-
706 micron particles. *Global Biogeochem Cy* 17.

707 Gordian, M.E., Ozkaynak, H., Xue, J.P., Morris, S.S., Spengler, J.D., 1996. Particulate air
708 pollution and respiratory disease in Anchorage, Alaska. *Environmental Health Perspectives* 104,
709 290-297.

710 Hacon, S., Ornelas, C., Ignotti, E., Longo, K., 2007. Fine particulate air pollution and hospital
711 admission for respiratory diseases in the Amazon region. *Epidemiology* 18, S81-S81.

712 Harley, R.A., Hannigan, M.P., Cass, G.R., 1992. Respeciation of Organic Gas Emissions and the
713 Detection of Excess Unburned Gasoline in the Atmosphere. *Environmental Science &*
714 *Technology* 26, 2395-2408.

715 Held, T., Ying, Q., Kleeman, M.J., Schauer, J.J., Fraser, M.P., 2005. A comparison of the
716 UCD/CIT air quality model and the CMB source-receptor model for primary airborne particulate
717 matter. *Atmospheric Environment* 39, 2281-2297.

718 Held, T., Ying, Q., Kaduwela, A., Kleeman, M., 2004. Modeling particulate matter in the San
719 Joaquin Valley with a source-oriented externally mixed three-dimensional photochemical grid
720 model. *Atmospheric Environment* 38, 3689-3711.

721 Hildemann, L.M., Markowski, G.R., Cass, G.R., 1991a. Chemical-Composition of Emissions
722 from Urban Sources of Fine Organic Aerosol. *Environmental Science & Technology* 25, 744-
723 759.

724 Hildemann, L.M., Markowski, G.R., Jones, M.C., Cass, G.R., 1991b. Submicrometer Aerosol
725 Mass Distributions of Emissions from Boilers, Fireplaces, Automobiles, Diesel Trucks, and
726 Meat-Cooking Operations. *Aerosol Science and Technology* 14, 138-152.

727 Hixson, M., Mahmud, A., Hu, J., Bai, S., Niemeier, D.A., Handy, S.L., Gao, S., Lund, J.R.,
728 Sullivan, D.C., Kleeman, M.J., 2010. Influence of regional development policies and clean
729 technology adoption on future air pollution exposure. *Atmospheric Environment* 44, 552-562.

730 Hixson, M., Mahmud, A., Hu, J., Kleeman, M.J., 2012. Resolving the interactions between
731 population density and air pollution emissions controls in the San Joaquin Valley, USA. *Journal*
732 *of the Air & Waste Management Association* 62, 566-575.

733 Hodzic, A., Madronich, S., Bohn, B., Massie, S., Menut, L., Wiedinmyer, C., 2007. Wildfire
734 particulate matter in Europe during summer 2003: meso-scale modeling of smoke emissions,
735 transport and radiative effects. *Atmospheric Chemistry and Physics* 7, 4043-4064.

736 Houck, J.E., et al., 1989. Determination of particle size distribution and chemical composition of
737 particulate matter from selected sources in California. Technical Report, Contract A6-175-32,
738 California Air Resources Board, OMNI Environment Service Incorporate, Desert Research
739 Institute, Beaverton, Oregon.

740 Hu, J., Howard, C.J., Mitloehner, F., Green, P.G., Kleeman, M.J., 2012. Mobile Source and
741 Livestock Feed Contributions to Regional Ozone Formation in Central California.
742 *Environmental Science & Technology* 46, 2781-2789.

743 Hu, J., Ying, Q., Chen, J.J., Mahmud, A., Zhao, Z., Chen, S.H., Kleeman, M.J., 2010. Particulate
744 air quality model predictions using prognostic vs. diagnostic meteorology in central California.
745 *Atmospheric Environment* 44, 215-226.

746 Hu, J., Zhang, H., Chen, S.-H., Vandenberghe, F., Ying, Q., Kleeman, M.J., 2014a. Predicting
747 Primary PM_{2.5} and PM_{0.1} Trace Composition for Epidemiological Studies in California.
748 *Environmental Science & Technology* 48, 4971-4979.

749 Hu, J., Zhang, H., Chen, S., Ying, Q., Vandenberghe, F., Kleeman, M.J., 2014b. Identifying
750 PM_{2.5} and PM_{0.1} Sources for Epidemiological Studies in California. *Environmental Science &*
751 *Technology* 48, 4980-4990.

752 Hu, J.L., Zhang, H. L., Chen, S. H., Wiedinmyer, C., Vandenberghe, F., Ying, Q., Kleeman, M.
753 J., Manuscript in preparation. Long-term Particulate Matter Modeling for Health Effects Studies
754 in California – Part II: Concentrations and Sources of Primary and Secondary Organic Aerosols.

755 Hughes, J., Tolsma, D., 2002. Association between particulate air pollution and acute respiratory
756 visits in an ambulatory care setting. *Epidemiology* 13, S125-S125.

757 Ito, K., Mathes, R., Ross, Z., Nadas, A., Thurston, G., Matte, T., 2011. Fine Particulate Matter
758 Constituents Associated with Cardiovascular Hospitalizations and Mortality in New York City.
759 *Environmental Health Perspectives* 119, 467-473.

760 Kan, H.D., Gu, D.F., 2011. Association Between Long-term Exposure to Outdoor Air Pollution
761 and Mortality in China: A Cohort Study. *Epidemiology* 22, S29-S29.

762 Kleeman, M.J., Cass, G.R., 1998. Source contributions to the size and composition distribution
763 of urban particulate air pollution. *Atmospheric Environment* 32, 2803-2816.

764 Kleeman, M.J., Cass, G.R., 2001. A 3D Eulerian source-oriented model for an externally mixed
765 aerosol. *Environmental Science & Technology* 35, 4834-4848.

766 Kleeman, M.J., Cass, G.R., Eldering, A., 1997. Modeling the airborne particle complex as a
767 source-oriented external mixture. *Journal of Geophysical Research-Atmospheres* 102, 21355-
768 21372.

769 Kleeman, M.J., Robert, M.A., Riddle, S.G., Fine, P.M., Hays, M.D., Schauer, J.J., Hannigan,
770 M.P., 2008. Size distribution of trace organic species emitted from biomass combustion and meat
771 charbroiling. *Atmospheric Environment* 42, 3059-3075.

772 Kleeman, M.J., Schauer, J.J., Cass, G.R., 1999. Size and composition distribution of fine
773 particulate matter emitted from wood burning, meat charbroiling, and cigarettes. *Environmental*
774 *Science & Technology* 33, 3516-3523.

775 Kleeman, M.J., Schauer, J.J., Cass, G.R., 2000. Size and composition distribution of fine
776 particulate matter emitted from motor vehicles. *Environmental Science & Technology* 34, 1132-
777 1142.

778 Kleeman, M.J., Ying, Q., Lu, J., Mysliwiec, M.J., Griffin, R.J., Chen, J.J., Clegg, S., 2007.
779 Source apportionment of secondary organic aerosol during a severe photochemical smog
780 episode. *Atmospheric Environment* 41, 576-591.

781 Krall, J.R., Anderson, G.B., Dominici, F., Bell, M.L., Peng, R.D., 2013. Short-term Exposure to
782 Particulate Matter Constituents and Mortality in a National Study of US Urban Communities.
783 *Environmental Health Perspectives* 121, 1148-1153.

784 Laden, F., Neas, L.M., Dockery, D.W., Schwartz, J., 2000. Association of fine particulate matter
785 from different sources with daily mortality in six US cities. *Environmental Health Perspectives*
786 108, 941-947.

787 Langrish, J.P., Bosson, J., Unosson, J., Muala, A., Newby, D.E., Mills, N.L., Blomberg, A.,
788 Sandstrom, T., 2012. Cardiovascular effects of particulate air pollution exposure: time course
789 and underlying mechanisms. *J Intern Med* 272, 224-239.

790 Laurent, O., Hu, J., Li, L., Cockburn, M., Escobedo, L., Kleeman, M., Wu, J., 2014. Sources and
791 contents of air pollution affecting term low birth weight in Los Angeles County, California,
792 2001-2008. *Environment Research Accepted for Publication*.

793 Laurent, O., Wu, J., Li, L., Chung, J., Bartell, S., 2013. Investigating the association between
794 birth weight and complementary air pollution metrics: a cohort study. *Environmental health* 12,
795 18.

796 Le Tertre, A., Medina, S., Samoli, E., Forsberg, B., Michelozzi, P., Boumghar, A., Vonk, J.M.,
797 Bellini, A., Atkinson, R., Ayres, J.G., Sunyer, J., Schwartz, J., Katsouyanni, K., 2002. Short-term
798 effects of particulate air pollution on cardiovascular diseases in eight European cities. *J*
799 *Epidemiol Commun H* 56, 773-779.

800 Levy, J.I., Diez, D., Dou, Y.P., Barr, C.D., Dominici, F., 2012. A Meta-Analysis and Multisite
801 Time-Series Analysis of the Differential Toxicity of Major Fine Particulate Matter Constituents.
802 *American Journal of Epidemiology* 175, 1091-1099.

803 Mahmud, A., Hixson, M., Hu, J., Zhao, Z., Chen, S. H., Kleeman, M. J., 2010. Climate impact
804 on airborne particulate matter concentrations in California using seven year analysis periods.
805 *Atmospheric Chemistry and Physics* 10, 11097-11114.

806 Mar, T.F., Norris, G.A., Koenig, J.Q., Larson, T.V., 2000. Associations between air pollution
807 and mortality in Phoenix, 1995-1997. *Environmental Health Perspectives* 108, 347-353.

808 Mass, C., Ovens, D., 2010. WRF model physics: progress, problems, and perhaps some
809 solutions. the 11th WRF Users' Workshop, 21-25 June, Boulder, CO.

810 Matsui, H., Koike, M., Takegawa, N., Kondo, Y., Griffin, R.J., Miyazaki, Y., Yokouchi, Y.,
811 Ohara, T., 2009. Secondary organic aerosol formation in urban air: Temporal variations and
812 possible contributions from unidentified hydrocarbons. *Journal of Geophysical Research:*
813 *Atmospheres* 114, D04201.

814 Michelson, S.A., Djalalova, I.V., Bao, J.-W., 2010a. Evaluation of the Summertime Low-Level
815 Winds Simulated by MM5 in the Central Valley of California. *Journal of Applied Meteorology*
816 *and Climatology* 49, 2230-2245.

817 Michelson, S.A., Djalalova, I.V., Bao, J.W., 2010b. Evaluation of the Summertime Low-Level
818 Winds Simulated by MM5 in the Central Valley of California. *Journal of Applied Meteorology*
819 *and Climatology* 49, 2230-2245.

820 Millstein, D.E., Harley, R.A., 2009. Revised estimates of construction activity and emissions:
821 Effects on ozone and elemental carbon concentrations in southern California. *Atmospheric*
822 *Environment* 43, 6328-6335.

823 Mysliwicz, M.J., Kleeman, M.J., 2002. Source apportionment of secondary airborne particulate
824 matter in a polluted atmosphere. *Environmental Science & Technology* 36, 5376-5384.

825 Ostro, B., Broadwin, R., Green, S., Feng, W.Y., Lipsett, M., 2006. Fine particulate air pollution
826 and mortality in nine California counties: Results from CALFINE. *Environmental Health*
827 *Perspectives* 114, 29-33.

828 Ostro, B., Feng, W.Y., Broadwin, R., Green, S., Lipsett, M., 2007. The effects of components of
829 fine particulate air pollution on mortality in California: Results from CALFINE. *Environmental*
830 *Health Perspectives* 115, 13-19.

831 Ostro, B., Lipsett, M., Reynolds, P., Goldberg, D., Hertz, A., Garcia, C., Henderson, K.D.,
832 Bernstein, L., 2010. Long-Term Exposure to Constituents of Fine Particulate Air Pollution and
833 Mortality: Results from the California Teachers Study. *Environmental Health Perspectives* 118,
834 363-369.

835 Pace, T.G., 2005. Methodology to Estimate the Transportable Fraction (TF) of Fugitive Dust
836 Emissions for Regional and Urban Scale Air Quality Analyses. US EPA August 2005.

837 Pope, C.A., Burnett, R.T., Thun, M.J., Calle, E.E., Krewski, D., Ito, K., Thurston, G.D., 2002.
838 Lung cancer, cardiopulmonary mortality, and long-term exposure to fine particulate air pollution.
839 *Jama-J Am Med Assoc* 287, 1132-1141.

840 Pope, C.A., Ezzati, M., Dockery, D.W., 2009. Fine-Particulate Air Pollution and Life
841 Expectancy in the United States. *New England Journal of Medicine* 360, 376-386.

842 Rasmussen, D.J., Hu, J., Mahmud, A., Kleeman, M.J., 2013. The Ozone–Climate Penalty: Past,
843 Present, and Future. *Environmental Science & Technology* 47, 14258-14266.

844 Robert, M.A., Kleeman, M.J., Jakober, C.A., 2007a. Size and composition distributions of
845 particulate matter emissions: Part 2- Heavy-duty diesel vehicles. *Journal of the Air & Waste
846 Management Association* 57, 1429-1438.

847 Robert, M.A., VanBergen, S., Kleeman, M.J., Jakober, C.A., 2007b. Size and composition
848 distributions of particulate matter emissions: Part 1 - Light-duty gasoline vehicles. *Journal of the
849 Air & Waste Management Association* 57, 1414-1428.

850 Sarnat, J.A., Sarnat, S.E., Crooks, J., Isakov, V., Touma, J., Ozkaynak, H., Mulholland, J.,
851 Russell, A., Kewada, P., 2011. Associations Between Spatially Resolved Estimates of Traffic-
852 related Pollution and Acute Morbidity: Assessing Agreement of Results Among Multiple
853 Exposure Assignment Approaches. *Epidemiology* 22, S31-S32.

854 Schauer, J.J., Kleeman, M.J., Cass, G.R., Simoneit, B.R.T., 1999a. Measurement of emissions
855 from air pollution sources. 1. C-1 through C-29 organic compounds from meat charbroiling.
856 *Environmental Science & Technology* 33, 1566-1577.

857 Schauer, J.J., Kleeman, M.J., Cass, G.R., Simoneit, B.R.T., 1999b. Measurement of emissions
858 from air pollution sources. 2. C-1 through C-30 organic compounds from medium duty diesel
859 trucks. *Environmental Science & Technology* 33, 1578-1587.

860 Schauer, J.J., Kleeman, M.J., Cass, G.R., Simoneit, B.R.T., 2001. Measurement of emissions
861 from air pollution sources. 3. C-1-C-29 organic compounds from fireplace combustion of wood.
862 *Environmental Science & Technology* 35, 1716-1728.

863 Schauer, J.J., Kleeman, M.J., Cass, G.R., Simoneit, B.R.T., 2002a. Measurement of emissions
864 from air pollution sources. 4. C-1-C-27 organic compounds from cooking with seed oils.
865 *Environmental Science & Technology* 36, 567-575.

866 Schauer, J.J., Kleeman, M.J., Cass, G.R., Simoneit, B.R.T., 2002b. Measurement of emissions
867 from air pollution sources. 5. C-1-C-32 organic compounds from gasoline-powered motor
868 vehicles. *Environmental Science & Technology* 36, 1169-1180.

869 Sickles II, J.E., Shadwick, D.S., 2002. Precision of atmospheric dry deposition data from the
870 Clean Air Status and Trends Network. *Atmospheric Environment* 36, 5671-5686.

871 Son, J.Y., Lee, J.T., Kim, K.H., Jung, K., Bell, M.L., 2012. Characterization of Fine Particulate
872 Matter and Associations between Particulate Chemical Constituents and Mortality in Seoul,
873 Korea. *Environmental Health Perspectives* 120, 872-878.

874 Stieb, D.M., Chen, L., Eshoul, M., Judek, S., 2012. Ambient air pollution, birth weight and
875 preterm birth: A systematic review and meta-analysis. *Environmental research* 117, 100–111.

876 Taback, H.J., Brienza, A.R., Macko, J., Brunetz, N., 1979. Fine particle emissions from
877 stationary and miscellaneous sources in the South Coast Air Basin. Technical Report, Contract
878 A6-191-30, California Air Resources Board, KVB Incorporate, Research-Cottrell, Tustin,
879 California.

880 Tainio, M., Juda-Rezler, K., Reizer, M., Warchałowski, A., Trapp, W., Skotak, K., 2012. Future
881 climate and adverse health effects caused by fine particulate matter air pollution: case study for
882 Poland. *Regional Environmental Change*, 1-11.

883 Tesche, T.W., Morris, R., Tonnesen, G., McNally, D., Boylan, J., Brewer, P., 2006.
884 CMAQ/CAMx annual 2002 performance evaluation over the eastern US. *Atmospheric*
885 *Environment* 40, 4906-4919.

886 Tran, H.T., Alvarado, A., Garcia, C., Motallebi, N., Miyasato, L., and Vance, W., 2008.
887 Methodology for Estimating Premature Deaths Associated with Long-term Exposure to Fine
888 Airborne Particulate Matter in California. Staff Report, California Environmental Protection
889 Agency, Air Resources Board.

890 Turpin, B.J., Lim, H.J., 2010. Species contributions to PM_{2.5} mass concentrations: revisiting
891 common assumptions for estimating organic mass. *Aerosol Science and Technology* 35:1, 602-
892 610.

893 U.S.EPA, 2007. Guidance on the Use of Models and Other Analyses for Demonstrating
894 Attainment of Air Quality Goals for Ozone, PM_{2.5} and Regional Haze, in: Agency, U.S.E.P.
895 (Ed.), Research Triangle Park, North Carolina.

896 Vineis, P., Hoek, G., Krzyzanowski, M., Vigna-Taglianti, F., Veglia, F., Airoidi, L., Autrup, H.,
897 Dunning, A., Garte, S., Hainaut, P., Malaveille, C., Matullo, G., Overvad, K., Raaschou-Nielsen,
898 O., Clavel-Chapelon, F., Linseisen, J., Boeing, H., Trichopoulou, A., Palli, D., Peluso, M.,
899 Krogh, V., Tumino, R., Panico, S., Bueno-De-Mesquita, H.B., Peeters, P.H., Lund, E.E.,
900 Gonzalez, C.A., Martinez, C., Dorronsoro, M., Barricarte, A., Cirera, L., Quiros, J.R., Berglund,
901 G., Forsberg, B., Day, N.E., Key, T.J., Saracci, R., Kaaks, R., Riboli, E., 2006. Air pollution and
902 risk of lung cancer in a prospective study in Europe. *Int J Cancer* 119, 169-174.

903 Volkamer, R., Jimenez, J.L., San Martini, F., Dzepina, K., Zhang, Q., Salcedo, D., Molina, L.T.,
904 Worsnop, D.R., Molina, M.J., 2006. Secondary organic aerosol formation from anthropogenic air
905 pollution: Rapid and higher than expected. *Geophysical Research Letters* 33, L17811.

906 Vukovich, J.M., Pierce, T., 2002. The Implementation of BEIS3 within the SMOKE modeling
907 framework. MCNC-Environmental Modeling Center, Research Triangle Park and National
908 Oceanic and Atmospheric Administration.

909 Walker, J.M., Philip, S., Martin, R.V., Seinfeld, J.H., 2012. Simulation of nitrate, sulfate, and
910 ammonium aerosols over the United States. *Atmos. Chem. Phys.* 12, 11213-11227.

911 Wang, K., Zhang, Y., Yahya, K., Wu, S.-Y., Grell, G., 2015. Implementation and Initial
912 Application of New Chemistry-Aerosol Options in WRF/Chem for Simulating Secondary
913 Organic Aerosols and Aerosol Indirect Effects for Regional Air Quality. *Atmospheric*
914 *Environment* doi:10.1016/j.atmosenv.2014.12.007.

915 Wei Wang, C.B., Michael Duda, Jimmy Dudhia, Dave Gill, Hui-Chuan Lin, John Michalakes,
916 Syed Rizvi, and Xin Zhang, January 2010. The Advanced Research WRF (ARW) Version 3
917 Modeling System User's Guide.

918 Wiedinmyer, C., Akagi, S.K., Yokelson, R.J., Emmons, L.K., Al-Saadi, J.A., Orlando, J.J., Soja,
919 A.J., 2011. The Fire INventory from NCAR (FINN): a high resolution global model to estimate
920 the emissions from open burning. *Geoscientific Model Development* 4, 625-641.

921 Willers, S.M., Eriksson, C., Gidhagen, L., Nilsson, M.E., Pershagen, G., Bellander, T., 2013.
922 Fine and coarse particulate air pollution in relation to respiratory health in Sweden. *European*
923 *Respiratory Journal* 42, 924-934.

924 William C. Skamarock, J.B.K., Jimmy Dudhia, David O Gill, Dale M. Barker, Michael G. Duda,
925 Xiang-Yu Huang, Wei Wang, and Jordan G. Powers, June 2008. A Description of the Advanced
926 Research WRF Version 3. NCAR Technical Note NCAR/TN-475+STR.
927 WRAP, 2005. 2002 Fire Emission Inventory for the WRAP Region –Phase II. Air Sciences Inc.
928 Ying, Q., Fraser, M.P., Griffin, R.J., Chen, J.J., Kleeman, M.J., 2007. Verification of a source-
929 oriented externally mixed air quality model during a severe photochemical smog episode.
930 Atmospheric Environment 41, 1521-1538.
931 Ying, Q., Kleeman, M.J., 2006. Source contributions to the regional distribution of secondary
932 particulate matter in California. Atmospheric Environment 40, 736-752.
933 Ying, Q., Lu, J., Allen, P., Livingstone, P., Kaduwela, A., Kleeman, M., 2008. Modeling air
934 quality during the California Regional PM10/PM2.5 Air Quality Study (CRPAQS) using the
935 UCD/CIT source-oriented air quality model - Part I. Base case model results. Atmospheric
936 Environment 42, 8954-8966.
937 Yu, S.C., Dennis, R., Roselle, S., Nenes, A., Walker, J., Eder, B., Schere, K., Swall, J., Robarge,
938 W., 2005. An assessment of the ability of three-dimensional air quality models with current
939 thermodynamic equilibrium models to predict aerosol NO₃⁻. Journal of Geophysical Research-
940 Atmospheres 110.
941 Zhang, H., Chen, G., Hu, J., Chen, S.-H., Wiedinmyer, C., Kleeman, M., Ying, Q., 2014a.
942 Evaluation of a seven-year air quality simulation using the Weather Research and Forecasting
943 (WRF)/Community Multiscale Air Quality (CMAQ) models in the eastern United States.
944 Science of The Total Environment 473–474, 275-285.
945 Zhang, H., DeNero, S.P., Joe, D.K., Lee, H.H., Chen, S.H., Michalakes, J., Kleeman, M.J.,
946 2014b. Development of a source oriented version of the WRF/Chem model and its application to
947 the California regional PM10 / PM2.5 air quality study. Atmos. Chem. Phys. 14, 485-503.
948 Zhang, H., Ying, Q., 2011. Secondary organic aerosol formation and source apportionment in
949 Southeast Texas. Atmospheric Environment 45, 3217-3227.
950 Zhang, H.L., Ying, Q., 2010. Source apportionment of airborne particulate matter in Southeast
951 Texas using a source-oriented 3D air quality model. Atmospheric Environment 44, 3547-3557.
952 Zhao, Z., Chen, S.H., Kleeman, M.J., Tyree, M., Cayan, D., 2011. The Impact of Climate
953 Change on Air Quality-Related Meteorological Conditions in California. Part I: Present Time
954 Simulation Analysis. Journal of Climate 24, 3344-3361.

955

956

957 **Figures and Tables**

958

959 Figure 1. Modeling domains (blue lines outline the CA_24km domain, and red lines outline the
960 SoCAB_4km (bottom) and SJV_4km domains (up)) and PM measurement sites (dots). Blue dots
961 represent the sites of the PM_{2.5} Speciation Trends Network (STN) and the State and Local Air
962 Monitoring Stations (SLAMS), green dots represent the Interagency Monitoring of Protected
963 Visual Environments (IMPROVE) sites, and gray dots represent the PM_{2.5} Federal Reference
964 Method (FRM) sites.

965

966 Figure 2. Monthly mean fractional bias (MFB) of PM_{2.5} EC, OC, nitrate, ammonium, sulfate, and
967 total mass. Solid lines represent the MFB criteria, and the blue dash lines represent the MFB
968 goals.

969

970 Figure 3. Monthly mean fractional errors (MFE) of PM_{2.5} EC, OC, nitrate, ammonium, sulfate,
971 and total mass. Solid lines represent the MFE criteria, and the blue dash lines represent the MFE
972 goals.

973

974 Figure 4. Mean fractional bias (MFB) and mean fractional errors (MFE) of PM and gaseous
975 species when calculated using daily, monthly and annual averages.

976

977 Figure 5. Predicted (red lines) vs. observed (dark dots) monthly average O₃ (a), CO (b), NO (c),
978 and PM_{2.5} ammonium (d) at Sacramento, Fresno, Bakersfield, Los Angeles, and Riverside.

979

980 Figure 6. Predicted (red lines) vs. observed (dark dots) monthly average PM_{2.5} nitrate (a), OC
981 (b), EC (c), and PM_{2.5} total mass (d) at Sacramento, Fresno, Bakersfield, Los Angeles, and
982 Riverside.

983

984 Figure 7. Monthly average NO concentrations adjusted with the predicted/observed CO ratios.
985 NO_noadj represents the NO concentrations in the UCD/CIT model predictions, and NO_adj
986 represents the NO concentrations adjusted with observations as:

987 $NO_{adj} = NO_{noadj} * CO_{predicted} / CO_{measured}$

988

989 Figure 8. Monthly average nitrate concentrations in 2008 at Sacramento and Fresno predicted
990 with perturbed relative humidity (RH+0.3), compared to the basecase nitrate predictions
991 (RH_ori) and observed concentrations (Obs)

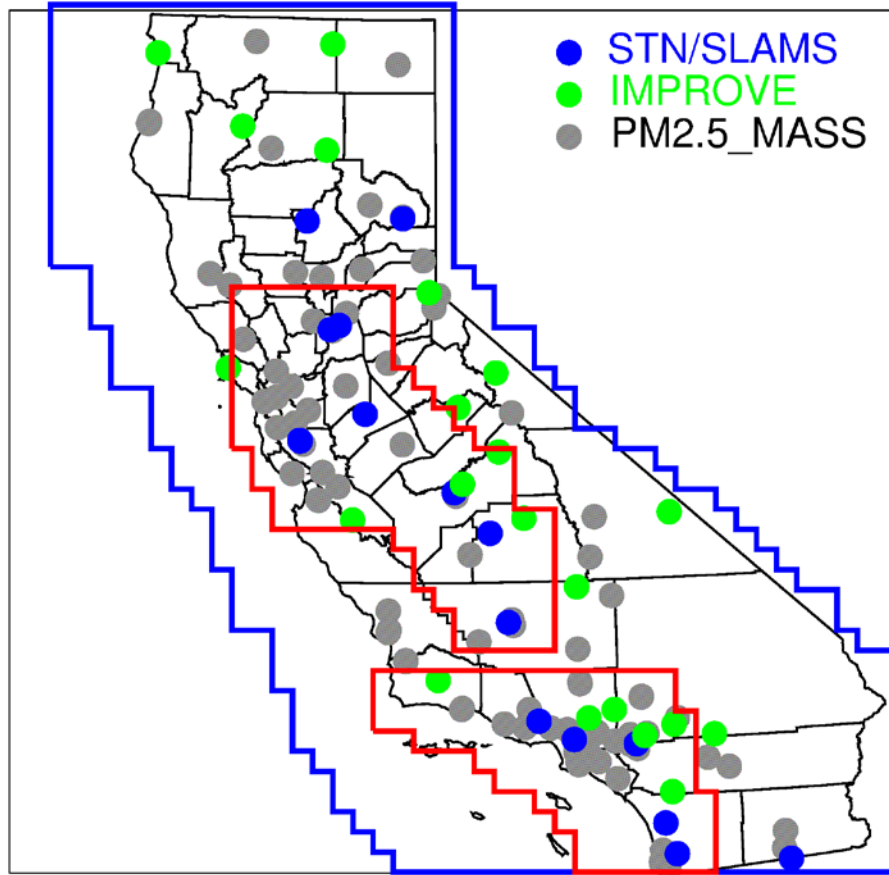
992

993 Figure 9. Association between predicted PM concentration bias and wind bias vs. observed
994 values. The observed PM concentrations and 1/u values on the x-axis are expressed in a relative
995 scale of 0-100% of maximum range calculated as $x (\%) = (C - C_{min}) / (C_{max} - C_{min}) * 100$. Values for
996 $[C_{min}, C_{max}]$ are listed in the concentration key. Bias between predicted vs. observed values is
997 shown on the y-axis. Ideal behavior is bias of zero at all concentrations & wind speeds.

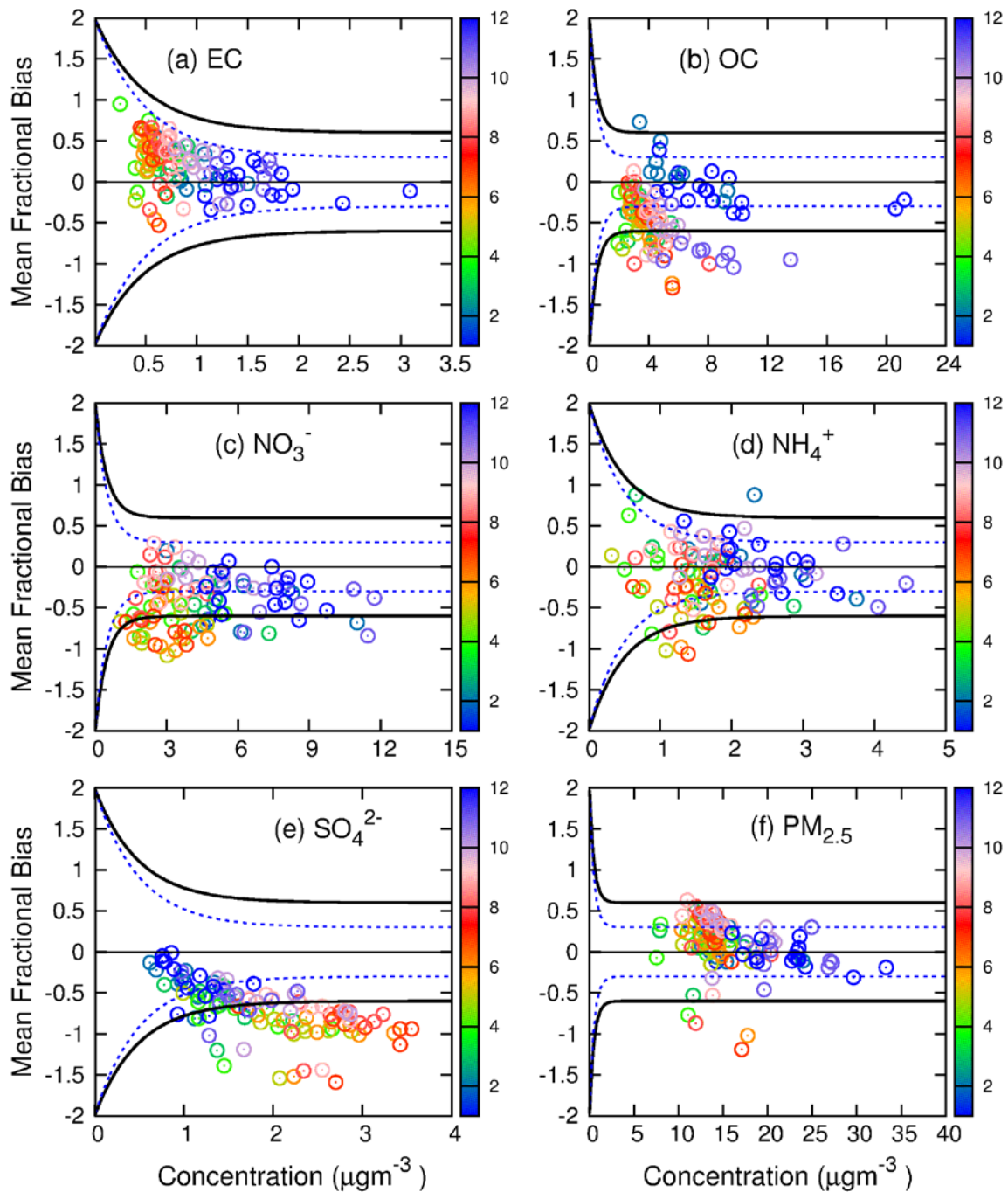
998

999 Figure 10. Predicted (1) vs. measured (2) 9-year average PM_{2.5} total mass (a), EC (b), OC (c),
1000 nitrate (d), sulfate (e), and ammonium (f) concentrations. The SoCAB_4km and SJV_4km
1001 results are overlaid on top of CA_24km results to create the model predicted spatial

1002 distributions. Predicted and measured concentrations of the same species are in the same scale
1003 showing in the panels of measurements
1004

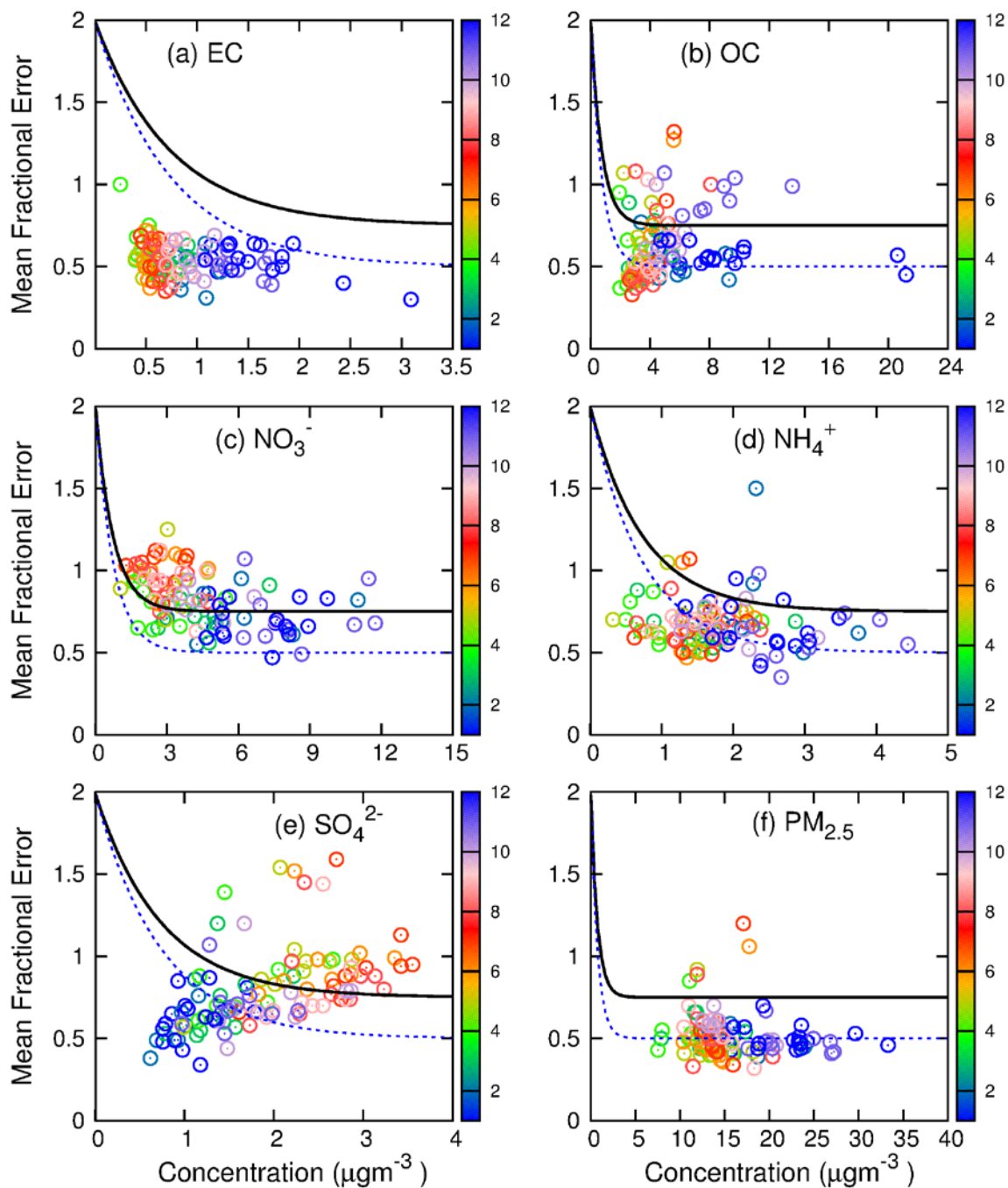


1005
 1006 Figure 1. Modeling domains (blue lines outline the CA_24km domain, and red lines outline the
 1007 SoCAB_4km (bottom) and SJV_4km domains (up)) and PM measurement sites (dots). Blue dots
 1008 represent the sites of the PM_{2.5} Speciation Trends Network (STN) and the State and Local Air
 1009 Monitoring Stations (SLAMS), green dots represent the Interagency Monitoring of Protected
 1010 Visual Environments (IMPROVE) sites, and gray dots represent the PM_{2.5} Federal Reference
 1011 Method (FRM) sites.



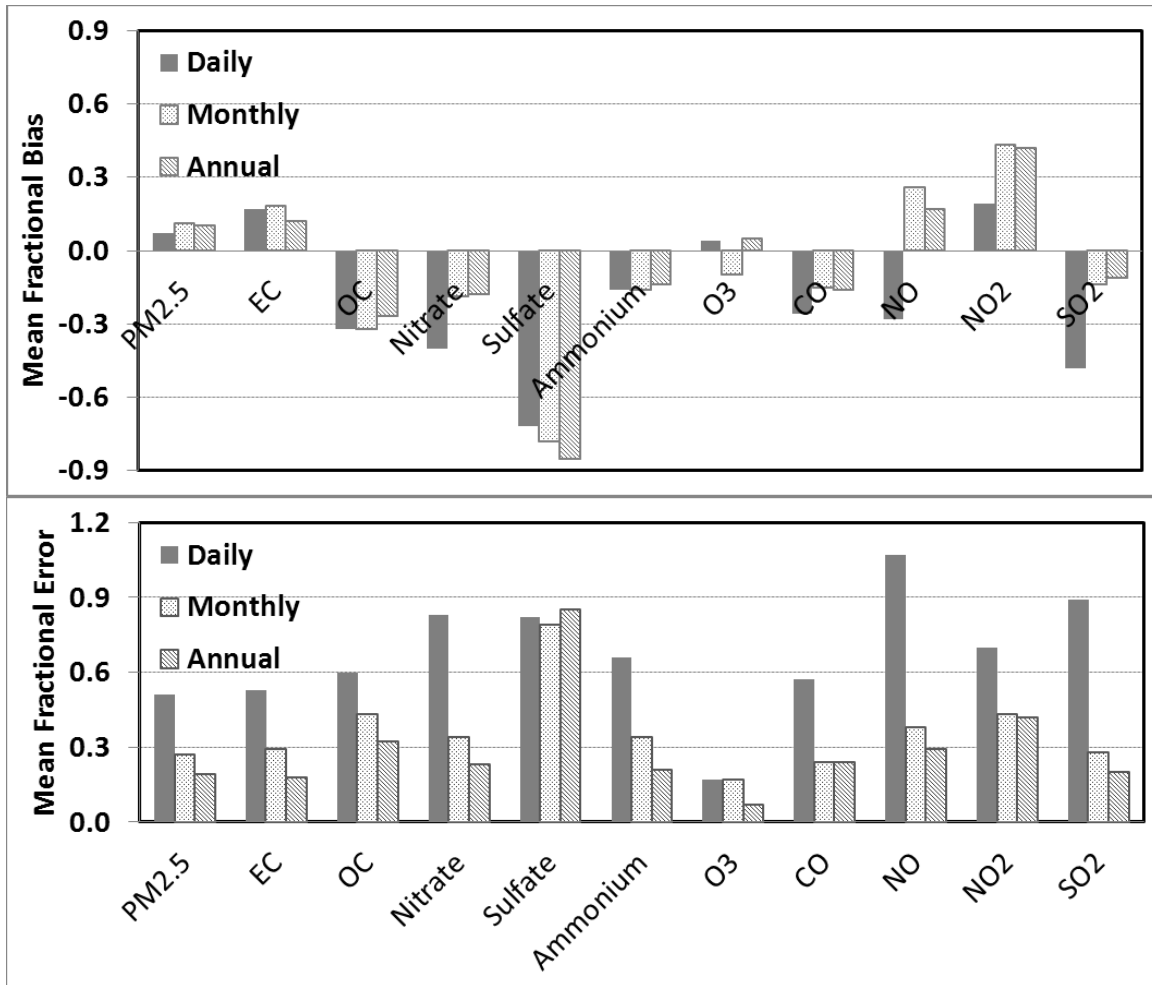
1012
 1013
 1014
 1015
 1016

Figure 2. Monthly mean fractional bias (MFB) of $\text{PM}_{2.5}$ EC, OC, nitrate, ammonium, sulfate, and total mass. Solid lines represent the MFB criteria, and the blue dash lines represent the MFB goals.



1017
 1018 Figure 3. Monthly mean fractional errors (MFE) of $\text{PM}_{2.5}$ EC, OC, nitrate,
 1019 and total mass. Solid lines represent the MFE criteria, and the blue dash lines represent the MFE
 1020 goals.
 1021

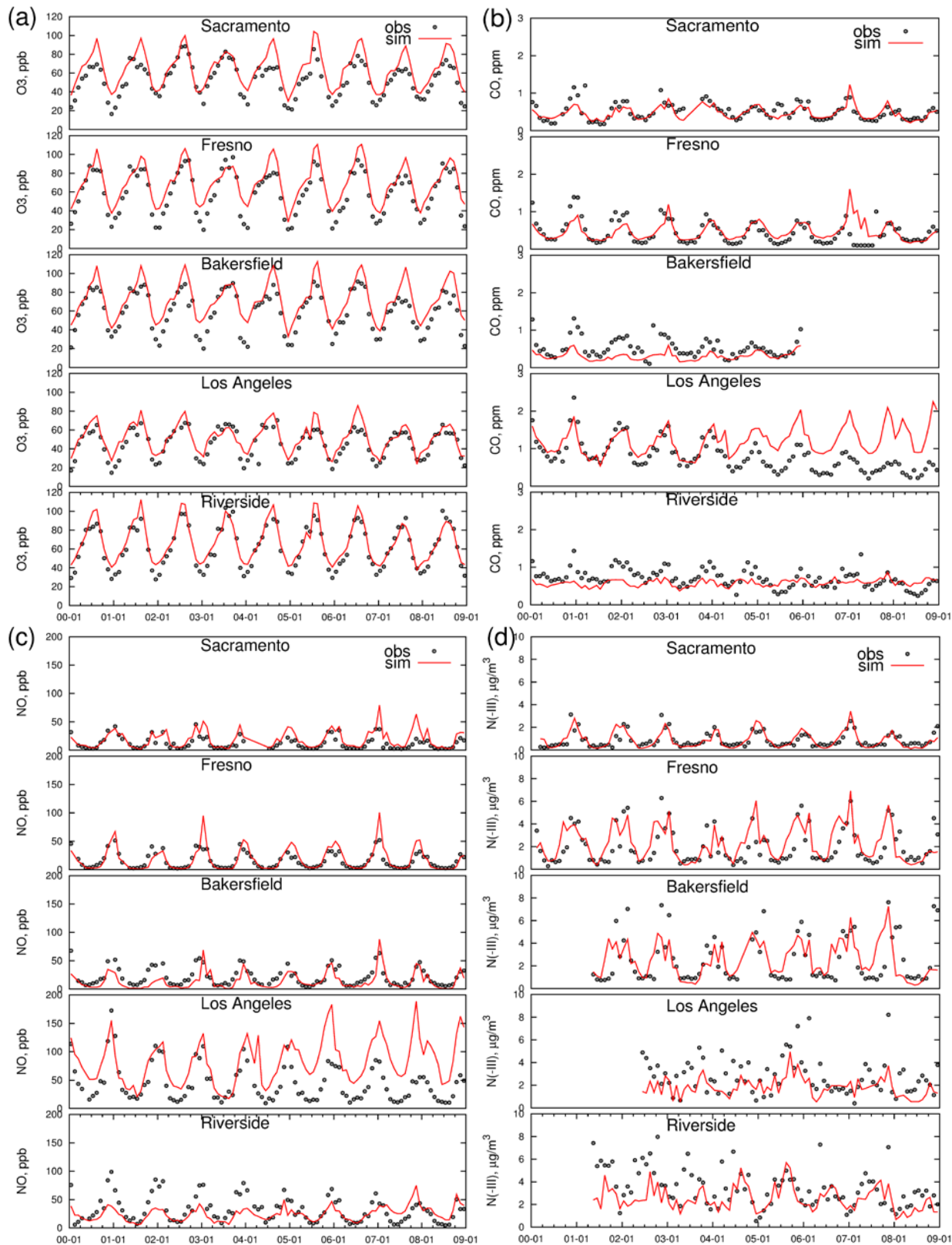
1022



1023
1024
1025
1026

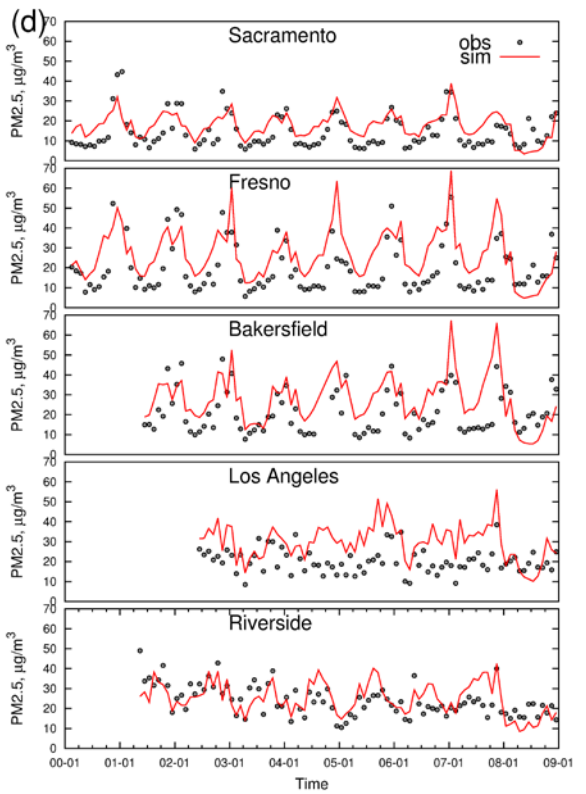
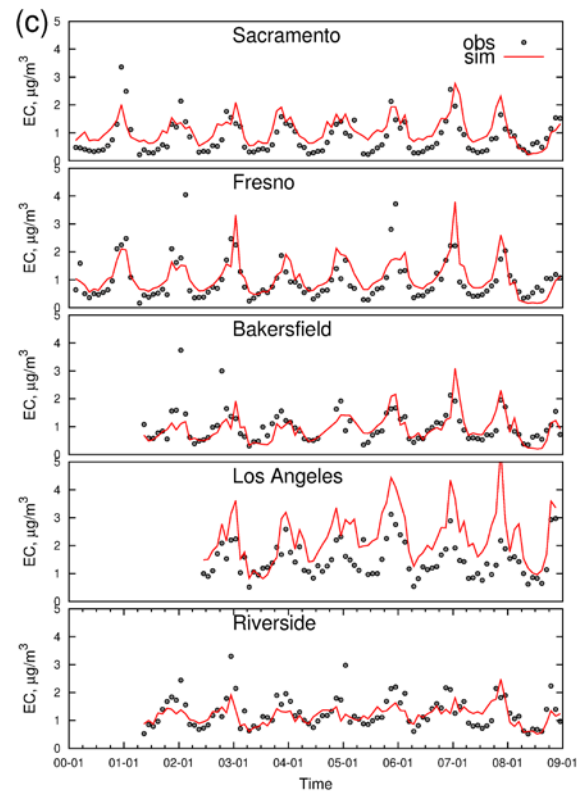
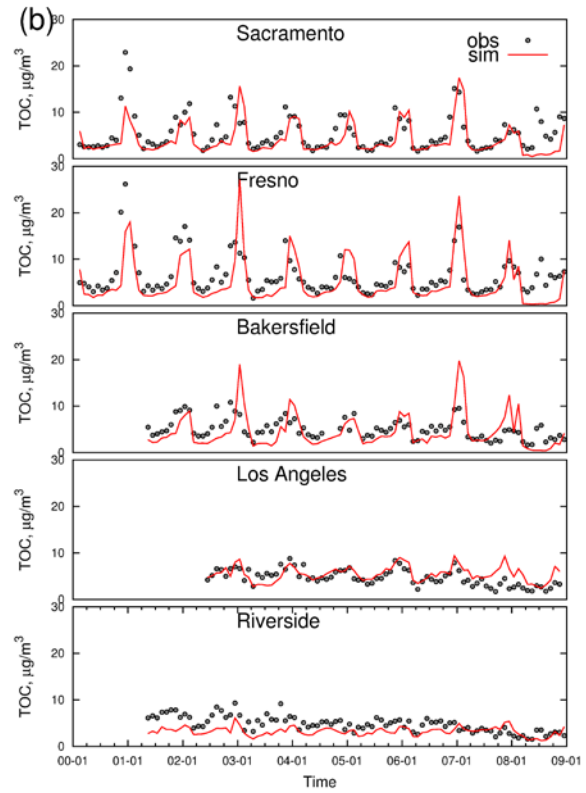
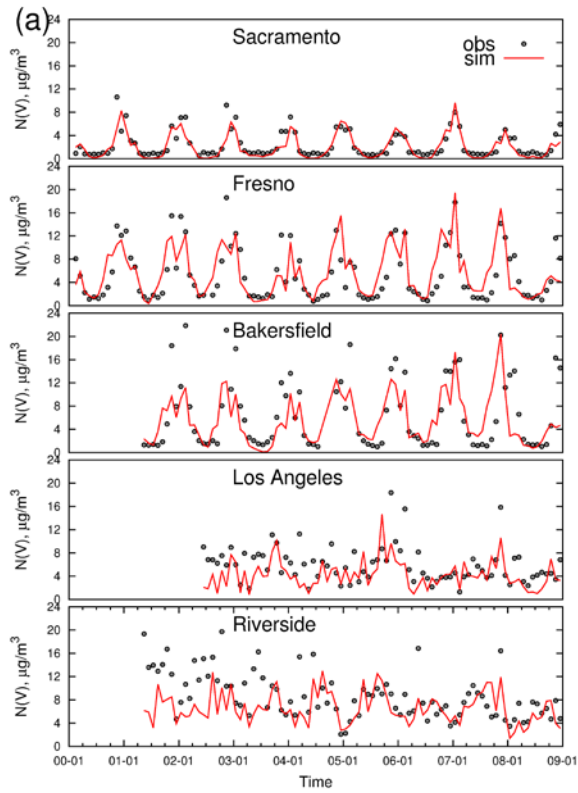
Figure 4. Mean fractional bias (MFB) and mean fractional errors (MFE) of PM and gaseous species when calculated using daily, monthly and annual averages.

1027



1028
1029
1030

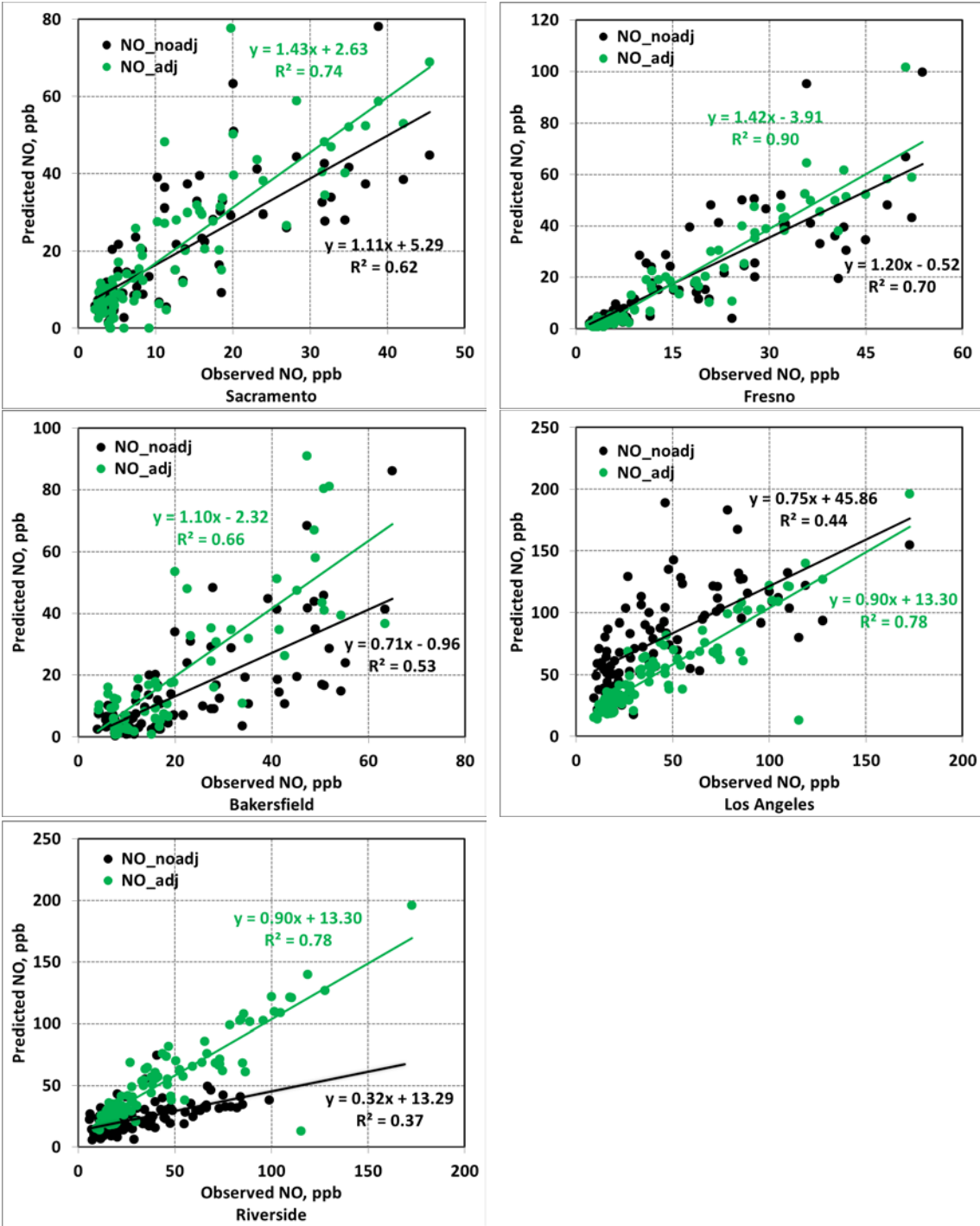
Figure 5. Predicted (red lines) vs. observed (dark dots) monthly average O₃ (a), CO (b), NO(c), and PM_{2.5} ammonium (d) at Sacramento, Fresno, Bakersfield, Los Angeles, and Riverside.



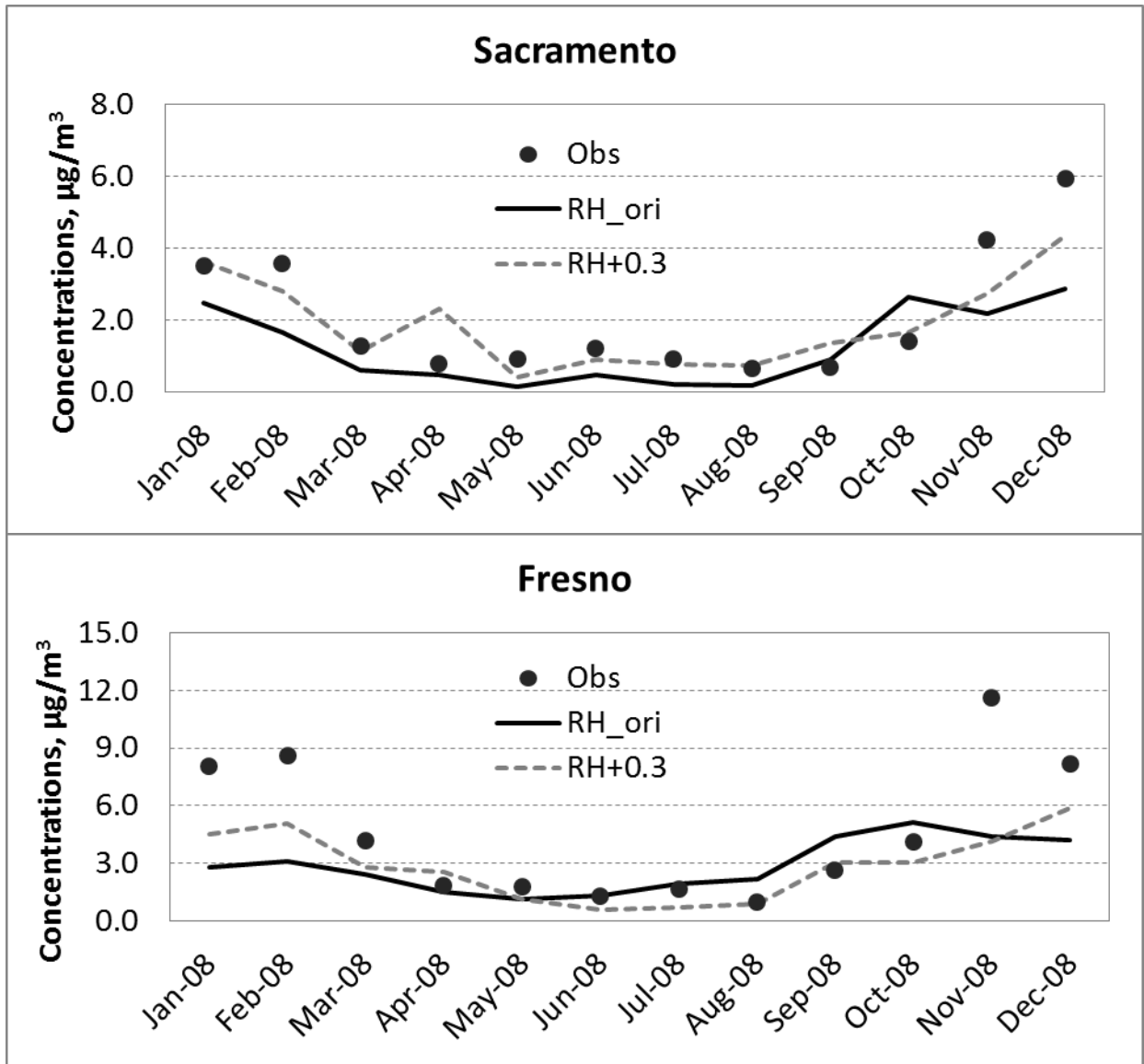
1031

1032
1033
1034
1035

Figure 6. Predicted (red lines) vs. observed (dark dots) monthly average PM_{2.5} nitrate (a), OC (b), EC (c), and PM_{2.5} total mass (d) at Sacramento, Fresno, Bakersfield, Los Angeles, and Riverside.



1036 Figure 7. Monthly average NO concentrations adjusted with the predicted/observed CO ratios.
 1037 NO_noadj represents the NO concentrations in the UCD/CIT model predictions, and NO_adj
 1038 represents the NO concentrations adjusted with observations as:
 1039 $NO_adj = NO_noadj * CO_predicted / CO_measured$
 1040



1041

1042
 1043
 1044
 1045
 1046

Figure 8. Monthly average nitrate concentrations in 2008 at Sacramento and Fresno predicted with perturbed relative humidity (RH+0.3), compared to the basecase nitrate predictions (RH_ori) and observed concentrations (Obs).

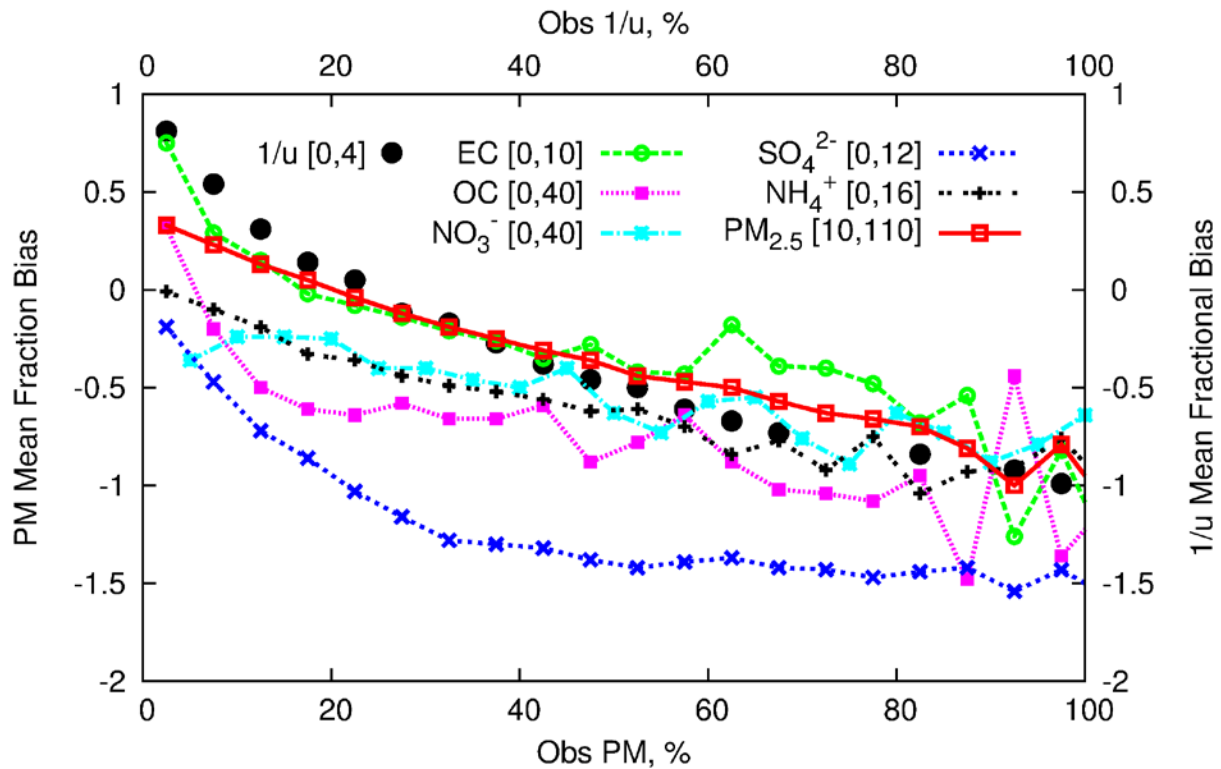


Figure 9. Association between predicted PM concentration bias and wind bias vs. observed values. The observed PM concentrations and $1/u$ values on the x-axis are expressed in a relative scale of 0-100% of maximum range calculated as $x (\%) = (C - C_{\min}) / (C_{\max} - C_{\min}) * 100$. Values for $[C_{\min}, C_{\max}]$ are listed in the concentration key. Units are $\mu\text{g m}^{-3}$ for concentrations, and m s^{-1} for wind speed. Bias between predicted vs. observed values is shown on the y-axis. Ideal behavior is bias of zero at all concentrations & wind speeds.

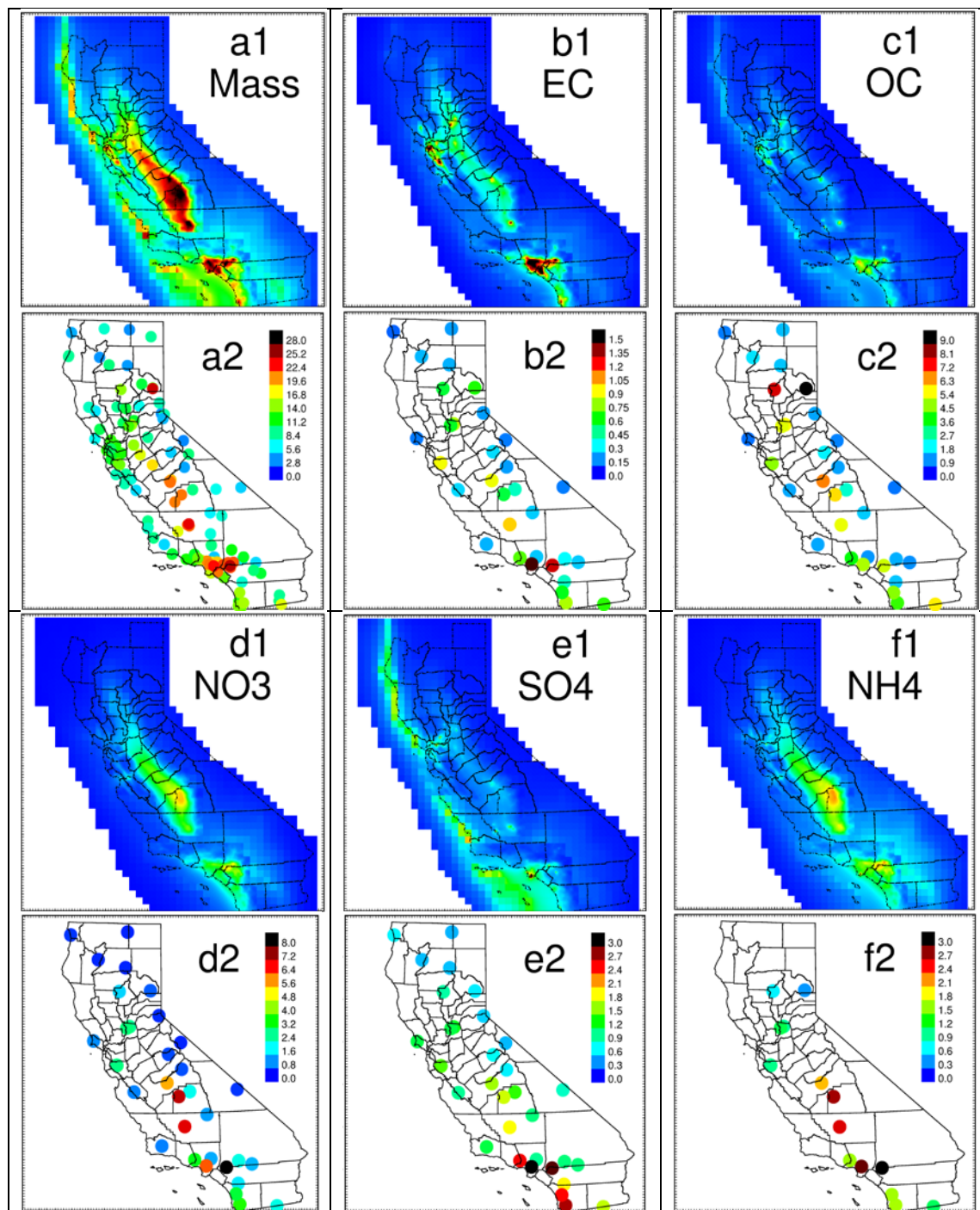


Figure 10. Predicted (1) vs. measured (2) 9-year average $PM_{2.5}$ total mass (a), EC (b), OC (c), nitrate (d), sulfate (e), and ammonium (f) concentrations. The SoCAB_4km and SJV_4km results are overlaid on top of CA_24km results to create the model predicted spatial distributions. Predicted and measured concentrations of the same species are in the same scale showing in the panels of measurements. Unit are $\mu g m^{-3}$.